Eur. Phys. J. A **3**, 25–48 (1998)

THE EUROPEAN PHYSICAL JOURNAL A

Nuclear levels in ^{228}Th populated in the decay of ^{228}Pa (II)

T. Weber[1], J. de Boer[2], K. Freitag[1], J. Gröger[1], C. Günther[1], P. Herzog[1], V.G. Soloviev[3], A.V. Sushkov[3], N.Yu. Shirikova[3]

[1] Institut für Strahlen- und Kernphysik, Universität Bonn, Nussallee 14-16, D-53115 Bonn, Germany
[2] Sektion Physik, Universität München, Am Coulombwall 1, D-85748 Garching, Germany
[3] Bogolubov Laboratory of Theoretical Physics, Joint Institute of Nuclear Research, 141980 Dubna, Russia

Received: 30 March 1998
Communicated by D. Schwalm

Abstract. The electron-capture decay of ^{228}Pa to levels in ^{228}Th was studied using mass-separated sources and a γ-ray detection system consisting of five Compton-suppressed Ge detectors. A total of 87 levels were observed up to an excitation energy of 2 MeV which are connected by approximately 500 γ-ray transitions. The complete octupole quadruplet, three excited $K^\pi = 0^+$ bands and two $K^\pi = 2^+$ bands were identified below 1.4 MeV. The observed level structure is compared to calculations within the quasiparticle-phonon nuclear model. The surprisingly good agreement indicates that ^{228}Th has less transitional character than hitherto assumed.

PACS. 23.20.-g Electromagnetic transitions – 21.60.Jz Hartree-Fock and random-physe approximations – 27.90.+b $220 \leq A$

1 Introduction

The nucleus ^{228}Pa decays by electron-capture with a half life of 22 h, populating a large number of excited levels in ^{228}Th up to an excitation energy of $\sim$ 2 MeV. The very complex decay was first studied using modern conversion-electron and γ-ray detection methods by Kurcewicz et al. [1]. More recently we restudied this decay with improved detection systems and mass-separated sources, yielding a level scheme for ^{228}Th with 52 excited levels connected by approximately 260 γ-ray transitions. This work was presented in [2] and discussed together with the corresponding level scheme observed in the ^{228}Ac decay [3].

The level scheme observed in these investigations can be devided into two parts: (1) A total of 23 levels below the threshold for two-quasiparticle excitations at $\sim$ 1.4 MeV. These levels were grouped into the ground band, the $K^\pi = 0^-$, 1^-, 2^- and 3^- octupole bands, two excited $K^\pi = 0^+$ and 2^+ bands and one tentative $K^\pi = 1^+$ band. While the octupole bands appeared to be well understood, the structure of the excited positive-parity bands remained largely unclear. (2) A total of 29 levels between $\sim$ 1.4 and $\sim$ 2 MeV. These levels could not be grouped into rotational bands and their structure remained unexplained.

While most of the assignments of the observed levels to rotational bands appeared to be safely established, one serious problem remained: for the $K^\pi = 1^-$ band only the 3^- member was proposed at 968 keV, but the 1^- and 2^- members expected below the 3^- level could not be identified. This indicated that an important aspect of the level scheme was still missed in the earlier investigations. Our studies of the ^{228}Pa decay [2] consisted in measurements of singles γ-rays and $e^- - \gamma$ coincidences only, and we therefore decided to restudy this decay with $\gamma - \gamma$ coincidences. These measurements lead to an unexpected solution for the $K^\pi = 1^-$ puzzle, and a confirmation and extension of the rotational bands proposed earlier. In the present work we give a detailed account of the new results, part of which had previously been published in a short note [4].

2 Experimental methods and results

2.1 Experimental details

Mass separated sources of the 22 h ^{228}Pa were prepared as described in [2]. Gamma-gamma coincidences were measured using an array of five Compton-suppressed HPGe detectors placed on the faces of a cube. This setup consists of two detector pairs placed at 180° to each other, and 8 pairs at 90°. In addition to the $\gamma - \gamma$ coincidences information on $\gamma - \gamma$ angular correlations could thus be obtained.

The $\gamma - \gamma$ coincidences were recorded in list-mode. Coincidence matrices were analysed for $\gamma - \gamma$ coincidences and angular correlations. A total of 2.8 million two-fold coincidences were recorded, with a suppression of the chance coincidences in the resulting coincidence spectra by factors of $\sim$ 200 to 300.

Table 1. Energies and intensities of γ-rays assigned to levels and transitions in ^{228}Th

Initial level E (keV)	I^π	E_γ(keV)[a]	I_γ^b
57.76	2^+	57.76 (2)	55 (3)
186.82	4^+	129.06 (2)	457 (23)
328.00	1^-	270.25 (2)	339 (17)
		328.03 (4) d	300 (30)
378.17	6^+	191.35 (2)	46.0 (23)
396.08	3^-	209.26 (2)	263 (13)
		338.32 (2)	817 (41)
519.20	5^-	141.00 (2)	20.8 (10)
		332.37 (2)	210 (11)
695.4	7^-	317.2 (3)	1.2 (6)
831.83	0^+	503.7 (2) d	7.4 (9)
		774.07	m
874.40	2^+	478.45 (4)	31.7 (17)
		546.45 (2)	28.0 (14)
		687.8 (2) d	4.8 (10)
		816.50 (12)	3.3 (4)
		874.5 (2)	7.7 (12)
938.6	0^+	610.7 (2)	2.4 (7)
		880.8	$\leq$ 2
944.20	1^-	547.8 (2)	1.6 (4)
		616.15 (5)	10.7 (8)
		886.44	$\leq$ 0.4
		944.31 (6)	9.8 (8)
968.33	2^-	572.3 (1) d	22.4 (24)
		640.33 (5) d	14 (2)
		910.6 (1) d	22 (2)
968.43	4^+	449.23 (3) d	22.5 (25)
		572.3 (1) d	38.9 (43)
		590.1 (3)	0.6 (2)
		781.9 (3) d	5.2 (12)
		910.7 (1) d	18 (3)
968.97	2^+	782.1 (1) d	35 (3)
		911.20 (2) d	2419 (120)
		968.98 (2)	1493 (75)
979.52	2^+	583.4 (1) d	18 (2)
		651.40 (5) d	15.9 (10)
		792.6 (2)	5.5 (6)
		921.6 (3) d	1.9 (4)
		979.3 (3)	4.2 (5)
1016.45	3^-	497.0 (2)	1.8 (4)
		620.27 (5)	14.1 (10)
		688.3 (1) d	8.3 (11)
		829.63	$\leq$ 1.4
		958.69 (11) d	44 (6)
		1016.45	$\leq$ 0.45
1022.53	3^+	835.65 (2) d	390 (25)
		964.80 (2) d	1202 (69)
1059.91	4^-	540.66 (5)	8.9 (6)
		663.92 (8) d	12 (2)
		873.0 (2)	16.6 (17)
1074.8	4^+	555.5 (1)	5.7 (6)
		678.6 (2)	5.1 (6)
		697.1 (4) d	0.9 (2)
		887.9 (3) d	1.5 (3)
		1017.0 (3)	2.1 (3)
1091.01	4^+	571.8 (2) d	0.6 (3)
		694.8 (2) d	2.6 (5)
		713.1 (3) d	4.8 (11)
		904.19 (3)	265 (13)
		1033.27 (7)	76 (4)
1120.1	0^+	1062.4 (1)	(1.5 (10))
1122.95	2^-	100.42	$\leq$ 5 g
		153.95 (2)	55 (3)
		178.7 (2)	0.7 (3)
		726.90 (10) d	42 (6)
		794.97 (2)	344 (17)
		1065.21 (7) d	10.3 (7)
1143.2	5^-	624.0 (2) d	1.4 (4)
		747.0 (4)	0.9 (3)
		764.5 (3) d	0.5 (2)
		956.6 (2) d	3 (1)
1153.48	2^+	174.02 (4)	3.0 (3)
		184.61 (5) d	1.7(2)
		209.28	(weak)
		214.9 (2) d	$\leq$ 1
		278.9 (1) d	4.1 (4)
		321.71 (3)	6.7 (4)
		966.66	$\leq$ 5
		1095.74 (14)	3.2 (6)
		1153.6 (3)	3.7 (8)
1168.37	3^-	77.36	$\leq$ 6 f
		145.82 (2)	25.7 (13)
		199.40 (2) d	45 (3)
		199.8 (2) d	1.8 (5)
		224.0 (2) d	1.7 (6)
		649.3 (1) d	5.1 (6)
		772.28 (2)	252 (13)
		840.36 (4)	159 (8)
		981.55	$\leq$ 1
		1110.55 (5) d	47 (5)
1174.52	5^+	796.2 (1)	16 (3)
		987.7 (1) d	33 (4)
1175.5	2^+	231.23	$\leq$ 0.2
		779.5 (6)	0.6 (3)
		847.1 (4)	0.5 (2)
		988.4 (1) d	9.9 (10)
		1117.3 (2)	4.4 (5)
		1175.4 (2)	2.3 (5)
1200.54	3^+	178.14 (7)	$\leq$ 2
		231.5 (1) d	1.0 (2)
		326.1 (3) d	2.5 (6)
		1013.54 (13) d	1.0 (5)
		1142.78 (15)	1.0 (3)
1226.57	4^-	135.51 (2)	10.4 (6)
		204.05 (2)	60 (3)
		258.1 (2) d	1.2 (6)
		258.1 (2) d	1.2 (6)
		282.37	(weak)
		707.40 (3)	79 (4)
		830.48 (3)	290 (15)
		1039.87 (6)	29.2 (15)
1261.5	4^+	170.6 (2)	1.0 (2)
		239.1 (3)	1.5 (4)
		292.5	$\leq$ 1
		293.1 (2)	1.3 (3)
		387.0 (3)	0.9 (3)
		883.4 (3)	1.1 (3)
		1074.7 (3) d	2.8 (5)
		1204.1 (3)	2.3 (3)
1270.0	6^+	891.8 (2) d	0.9 (3)
1290.2	4^+	911.7 (1) d	8 (4)
		1103.4 (1)	4.4 (4)
1297.37	5^-	206.3 (1)	5.0 (7)
		602.0	$\leq$ 2
		778.1 (2)	27 (3)
		901.4 (3) d	20 (3)
		1110.55 (5) d	24 (2)
1344.1	3^-	168.4 (3)	0.6 (3)
		825.1 (2)	1.4 (3)
		948.0 (2)	2.7 (5)
		1016.1 D	$\leq$ 0.7
		1157.3 D	$\leq$1$\leq$ 1
		1286.3 D	$\leq$ 2
1393.4	1^+,2,3^-	425.0 (2)	1.6 (3)
		449.2 (1) d	2.5 (9)
		1065.4 (4) d	1.1 (4)
1416.0	2^+,3^-	399.8 (2)	3.5 (4)
		447.6 (2)	1.3 (5)
		471.8 (2)	3.9 (9)
		1019.9 D	m
		1088.0 D	$\leq$ 1
		1229.2 D	$\leq$ 1.5
		1358.3 (3)	3.4 (5)
1431.98	4^+	134.9 (2)	2.0 (8)
		161.6 (4)	0.8 (3)
		231.4 (1) d	8.3 (5)
		257.49 (2)	14.0 (7)
		263.62 (2)	21.7 (11)
		278.5 (1) d	16 (2)
		288.9 (1)	$\leq$ 2
		340.98 (2)	205 (10)
		357.1 (2) d	(3.7 (4))
		372.2 (2) d	0.9 (3)

Table 1. *(continued)*

Table 1. *(continued)*

Initial level E (keV)	I^π	E_γ(keV)[a]	I_γ^b
		409.45 (2)	1000 (50)
		415.6 (1) d	4.8 (5)
		452.52 (6)	10.2 (8)
		463.02 (2) d	2221 (112)
		463.3 (1) d	16 (4)
		557.4 (1)	5.5 (6)
		1053.8 (1) d	3.6 (14)
		1245.17 (6)	56 (3)
		1374.26 (7)	∼10
1448.8	$3,4^-$	389.1 (2) d	$\leq$ 4
		432.5 (3) d	$\leq$ 3
		480.6 (2) d	$\leq$ 3
		1052.7 (2) d	$\leq$ 3
		1261.7 (4)	$\leq$ 1.5
1450.39	4^-	18.41	45 (7) h
		153.02 (2)	11.1 (6)
		223.80 (2) d	131 (7)
		275.85 (4)	8.2 (7)
		282.01 (2)	186 (9)
		327.45 (4) d	310 (30)
		359.36 (3)	13.0 (7)
		390.45 (5) d	11.1 (6)
		427.90 (3)	12.4 (8)
		434.01 (3)	17.3 (10)
		482.03 (5) d	15.1 (8)
		931.1 (2) d	3.9 (7)
		1054.23 (6) d	33 (3)
1497.7	$4^+,5^-$	354.5 (2)	∼ 1
		481.4 (2) d	3.3 (9)
		529.0 (3) d	0.5 (2)
		978.3 (3)	1.6 (6)
		1119.5 (3)	1.0 (4)
		1310.8 (1)	4.8 (5)
1531.47	3^+	99.47 (6)	18 (3)
		356.95	$\leq$ 0.4
		377.99	$\leq$ 2
		440.4 (2)	2.2 (6)
		509.13 (8)	7 (1)
		562.50 (4)	14.0 (8)
		1135.39	$\leq$ 1
		1344.65	$\leq$ 1
1581.0	(2^-)	354.43	$\leq$ 0.8
		601.48	$\leq$ 0.4
		1184.71 (9)	4.7 (4)
		1252.98 (10)	6.8 (6)
		1523.4 (2) d	4.6 (8)
1588.33	4^-	56.86 (3)	10.6 (5)
		137.95 (2)	66 (3)
		156.34 (2)	13.6 (7)
		420.03 (8)	6.8 (5)
		465.4 (1) d	12 (2)
		528.5 (2) d	0.9 (2)
1638.26	2^+	469.9 (5) d	1.4 (8)
		515.20 (11) d	2.1(10)
		1310.26	$\leq$ 0.2
		1451.44	$\leq$ 0.5
		1580.5 (3)	21.8 (14)
		1638.30 (7) d	18.8 (11)
1643.15	$(2,3)^-$	299.0 (2) d	(1.3 (6))
		416.5 (1) d	2.7 (5)
		474.7 (3)	7 (2)
		520.17 (8)	9.2 (10)
		583.2 (2) d	1.2 (3)
		626.7 (1)	4.9 (9)
		674.7 (2) d	2.1 (7)
		698.9 (1)	6.3 (10)
		1247.07 (5)	82 (4)
		1315.2 (2)	2.0 (5)
1643.8	$(2,3,4)^+$	442.9 (3) d	∼ 1.0 (5)
		490.4 (2)	8.2 (4)
		552.9 (2)	1.8 (4)
		621.4 (1) d	9.2 (10)
		674.7 (1) d	25 (3)
1645.92	3^+	114.49 (10)	1.0 (2)
		229.9 (4) d	(1.6 (6))
		419.3 (2)	2.8 (5)
		444.9 (3) d	∼ 1.0 (5)
		470.6 (2) d	(1.2 (5))

Table 1. *(continued)*

Initial level E (keV)	I^π	E_γ(keV)[a]	I_γ^b
		477.5 (1) d	3.4 (5)
		492.22 (10)	2.8 (3)
		523.16 (11) d	11 (2)
		554.8 (1)	4.0 (4)
		571.1 (1) d	(5.7 (25))
		586.2 (2)	1.2 (3)
		623.7 (2) d	1.3 (4)
		629.4 (2)	3.7 (6)
		666.47 (4) d	6.8 (8)
		676.9 (2)	8.0 (15)
		1249.7 (2)	7.3 (10)
		1459.2 (2)	86 (5)
		1588.15 (5)	372 (19)
1667.3		1148.2 (2) d	2.1 (5)
		1480.5 (2) d	5.0 (14)
1678.4	$2,3,4^+$	503.0 (2) d	(0.6 (2))
		803.8 (2)	0.8 (4)
		1282.6 (4)	0.9 (3)
		1620.67 (10) d	46 (2)
1682.71	$2^+,3,4^+$	660.18	$\leq$ 2
		1286.3 (3) d	2.5 (8)
		1496.15 (6) d	24.4 (20)
		1625.0 (2)	7.0 (14)
1683.77	(4^-)	457.38 (6)	3.0 (3)
		515.1 (1) d	3.6 (6)
		623.7 (2) d	1.4 (3)
		667.5 (3)	1.6 (5)
		1164.58 (7)	13.2 (7)
		1287.79 (8)	15.6 (11)
1688.39	$(2,3)^+$	42.47	$\leq$ 1
		671.94	$\leq$ 1
		813.93	$\leq$ 0.5
		1501.5 (2)	7.4 (6)
		1630.63 (6)	26.5 (13)
1707.2	2.3^-	1311.6 (4)	0.8 (3)
		1379.2 (2)	3.1 (15)
1724.28	2^+	308.2 (2)	(4.5 (15))
		497.71	$\leq$ 0.4
		523.5 (1) d	5 (1)
		548.74 (11)	(4.1 (5))
		570.88 (4) d	28 (3)
		604.2 (1)	4 (1)
		701.72 (4)	37.6 (21)
		755.32 (2) d	192 (10)
		780.2 (3) d	1.0 (3)
		849.5 (2) d	1.0 (4)
		1537.8 (2) d	7.3 (10)
		1666.53 (6)	33.5 (17)
		1724.0 (2)	5.0 (5)
1735.7	$2^+,3,4^+$	1548.7 (4) d	∼ 3.0 (15)
		1677.9 (1)	6.5 (5)
1743.88	4^+	590.40	$\leq$ 1
		683.97	$\leq$ 0.6
		727.2 (3) d	0.7 (2)
		764.3 (3) d	1.2 (5)
		1347.6 (3)	1.6 (5)
		1365.72 (12)	4.0 (4)
		1415.8 (2)	3.2 (7)
		1557.06 (6)	44.2 (22)
		1686.15 (7)	23.9 (12)
1757.9	$1^-,2,3^-$	741.9 (3) d	1.4 (5)
		1361.4 (5)	1.2 (5)
		1430.0 (3)	1.9 (7)
1760.25	$(2,3)^+$	416.15	$\leq$ 0.3
		584.75	$\leq$ 0.4
		668.9 (2)	2.2 (7)
		737.8 (2)	7.4 (13)
		791.43 (9) d	2.3 (3)
		1573.3 (3) d	5.6 (10)
		1702.6 (3)	11.5 (11)
1796.4	$3^+,4,5^+$	621.9 (2) d	1.6 (5)
		705.3 (2)	6 (2)
		1609.6 (1)	9.2 (7)
1802.9	$1^-,2,3^-$	1406.8 (2)	3.2 (8)
		1474.8 (4)	0.9 (5)
1804.60	(4^+)	116.26 (5)	1.6 (2)
		121.18 (7)	1.9 (3)

Table 1. *(continued)*

Initial level E (keV)	I^π	E_γ(keV)[a]	I_γ^b
		121.87 (3)	3.3 (3)
		158.74 (3)	12.5 (7)
		216.3 (1)	11 (3)
		354.21	$\leq$ 1.6
		372.60 (3) d	14.8 (9)
		651.5 (2) d	3.4 (5)
		713.6 (2) d	1.0 (5)
		781.8 (1) d	6.8 (9)
		835.63	m
		1286.0 (3) d	1.4 (5)
		1426.43	$\leq$ 0.3
		1618.0 (1)	9.0 (6)
		1746.84	$\leq$ 3
1811.5	1^-,2,3^-	1415.5 (2)	6 (1)
		1483.5 (2) d	3.5 (11)
1817.43	4^-	229.3 (2) d	2.9 (17)
		367.04 (2)	24.5 (12)
		590.7 (1)	3.3 (7)
		642.7 (2)	2.8 (8)
		649.0 (1) d	5.9 (8)
		674.6 (3) d	$\leq$ 2
		694.5 (1) d	5 (1)
		726.3 (2) d	1.9 (6)
		757.4 (2)	1.9 (5)
		801.1 (1) d	4.6 (5)
		1298.3 (2)	4.5 (4)
		1421.1 (2)	12.5 (9)
1823.4	3^-,4,5	596.8 (2)	1.5 (4)
		732.9 (4)	0.7 (3)
		1304.2 (3)	0.7 (3)
1842.2	2^+,3^-	751.1 (2)	1.8 (7)
		819.9 (2)	1.7 (5)
		862.8 (3)	1.1 (4)
		1513.4 (5) d	0.6 (2)
		1784.4 (2)	6.2 (5)
1864.8	1^-,2,3^-	696.5 (2) d	2.4 (5)
		741.8 (2) d	4.0 (6)
		895.9 (1)	14.1 (7)
		990.3 (2)	2.2 (6)
		1468.8 (3)	2.8 (7)
		1536.8 (3) d	1.4 (5)
		1807.2 (1)	6.0 (5)
		1865.1 (1)	8.0 (4)
1876.5	3^-,4,5^-	1357.2 (3)	1.5 (5)
		1480.4 (3) d	1.3 (6)
1879.0	3^-,4,5^-	1359.9 (3)	1.3 (5)
		1482.9 (3) d	2.0 (6)
1892.99	3^+	157.5 (2)	1.8 (5)
		214.6 (1) d	$\leq$ 1
		255.2 (3) d	0.6 (2)
		444.0 (2) d	$\sim$ 5 (1)
		477.1 (3) d	(3.0 (5))
		666.47 (4) d	18.3 (9)
		692.47 (7)	20.1 (15)
		718.0 (2) d	1.6 (6)
		724.5 (1) d	5.7 (9)
		739.2 (2)	5.7 (9) c
		770.2 (2) d	22.8 (15)
		801.7 (3) d	1.1 (4)
		870.45 (2)	159 (8)
		876.7 (2) d	2.1 (8)
		913.3 (2)	3.9 (13)
		924.0 (1) d	16 (2)
		924.5 (1) d	10 (3)
		924.6 (1) d	5 (2)
		1018.5 (1)	13 (3)
		1706.16 (7)	28.4 (14)
		1835.26 (5)	98 (5)
1899.98	2^+	253.9 (5)	0.5 (2)
		261.6 (2)	1.1 (4)
		506.5 (2)	$\leq$ 2
		724.7 (3) d	(1.0 (5))
		780.0 (3)	1.9 (9)
		877.35 (7) d	8.0 (10)
		883.53	$\leq$ 0.5
		920.46	$\leq$ 1
		931.02 (7) d	6.5 (6)
		1503.7 (2)	7.2 (6)

Table 1. *(continued)*

Initial level E (keV)	I^π	E_γ(keV)[a]	I_γ^b
		1572.0 (1) d	4 (1)
		1713.16	$\leq$ 1
		1842.15 (8)	22.9 (12)
		1900.3 (3)	3.4 (5)
1901.90	4^+	255.9 (2) d	1.4 (6)
		640.3 (2) d	$\sim$ 1.2 (5)
		810.7 (2)	1.2 (4)
		826.6 (3) d	(2 (1))
		933.1 (3)	2.5 (10)
		1383.2 (2)	5.5 (5)
		1505.9 (2)	5.5 (5)
		1523.5 (2) d	1.4 (6)
		1715.06 (10)	5.0 (3)
1908.4	(3^-)	785.7 (2)	2.0 (6)
		817.4 (3)	1.0 (3)
		848.6 (2)	0.8 (3)
		885.7 (2)	1.9 (4)
		891.9 (2) d	2.0 (7)
		939.9 (2)	2.3 (5)
		964.3 (3) d	3.0 (13)
		1512.9 (3) d	1.4 (5)
1924.1	2^-,3,4	697.6 (1) d	4.8 (8)
		723.6 (1)	6 (1)
		755.7 (1) d	4.2 (10)
1924.6	$(4,5^+)$	750.10 (10)	6.7 (8)
		902.1 (5) d	3 (1)
		1405.5 (2)	3.2 (8)
1925.20	4^+	476.7 (2) d	$\sim$ 1.0 (5)
		663.5 (2) d	$\sim$ 2.8 (5)
		724.42 (11)	7.6 (9)
		771.72	$\leq$ 1
		834.1 (1) d	25 (4)
		850.5 (2) d	(3.3 (15))
		865.2 (2)	0.6 (2)
		908.7 (3)	2.9 (9)
		956.8 (2) d	22 (5)
		1529.02 (6)	26.1 (13)
		1547.0 (2)	4.4 (12)
		1738.48 (5)	96 (5)
1928.54	3^+	168.29	$\leq$ 1
		584.4	$\leq$ 0.3
		775.06	$\leq$ 1
		837.0 (1) d	4.5 (10)
		906.0 (6)	1.7 (6)
		1741.6 (2)	4.2 (8)
		1870.80 (9)	7.3 (4)
1938.9	4	677.8 (2)	$\sim$ 1.1 (4)
		764.0 (3) d	1.8 (10)
		847.8 (3)	0.5 (2)
		879.1 (3)	0.6 (2)
		916.6 (3)	1.7 (5)
		1419.8 (2)	2.0 (9)
		1542.8 (2)	2.8 (5)
		1752.1 (2)	3.7 (4)
1944.88	3^+	148.4 (2)	3 (1)
		184.61 (5) d	4.5 (4)
		220.61 (2)	12.4 (6)
		237.7 (3)	1.8 (8)
		299.10 (10) d	3.0 (8)
		306.61 (2)	20.0 (10)
		512.79 (11)	13.3 (13)
		551.3 (2)	$\leq$ 2
		683.4 (2)	$\sim$ 1.0(4)
		718.31 (2) d	62 (3)
		744.2 (1)	3.5 (10)
		769.6 (1) d	(4 (2))
		776.52 (3)	79 (4)
		791.43 (9) d	36 (4)
		853.97 (8)	8.2 (7)
		922.5 (2) d	20.6 (21)
		928.4 (2) d	8.9 (8)
		965.3 (2) d	12 (2)
		976.00 (5) d	124 (10)
		976.5 (1) d	6 (2)
		976.5 (1) d	7 (3)
		1000.68	$\leq$ 0.1
		1070.40 (7)	12.0 (8)
		1548.8	m

Table 1. *(continued)*

Initial level E (keV)	I^π	E_γ(keV)[a]	I_γ^b
		1758.11 (5)	90 (5)
		1887.13 (5)	240 (12)
1945.8	4^+,5^-	1426.6 (1)	4.8 (6)
		1549.3 (2) d	12 (2)
		1567.6 (3)	2.3 (11)
1949.7	1^+,2,3^-	827.1 (3) d	2.5 (8)
		927.2 (2) d	2.8 (5)
		980.7 (2)	1.5 (5)
		1005.5 (2)	1.2 (4)
		1075.1 (2) d	1.4 (4)
1958.3	(2^+)	935.8 (2)	2.6 (5)
		1561.7 (4)	1.0 (4)
		1958.1 (2)	2.9 (3)
1964.90	(2^+)	321.75	(weak)
		548.9	$\leq$ 0.8
		1778.0 (6)	0.6 (2)
		1907.13 (11)	9.9 (5)
		1965.22 (12) d	4.3 (4) u
1974.20	4^+	1455.0 (2)	11.6 (7)
		1578.2 (2)	13.3 (13)
		1595.8 (3)	1.9 (8)
		1787.2 (2)	3.7 (4)
		1916.6 (3)	1.5 (3)
1981.97	3,4^+	684.6 (3)	1.4 (6)
		890.6 (3)	1.0 (3)
		959.1 (1) d	5.9 (8)
		1013.54 (13) d	3 (1)
		1013.64	$\leq$ 0.2
		1585.5 (2)	3.2 (10)
		1795.15 (6)	11.9 (7)
		1924.2 (2)	1.8 (2)
2010.14	2^+,3	371.88	$\leq$ 0.2
		887.2 (2) d	2.5 (8)
		919.1 (2)	3.6 (9)
		1040.9 (2)	5.8 (11)
		1823.19 (10)	4.7 (3)
		1952.39 (10)	7.6 (5)
2016.75	4^+,5^-	1048.2 (3)	1.3 (5)
		1497.5 (2) d	3.0 (2)
		1620.67 (10) d	2.9 (8)
		1638.5 (3) d	0.9 (4)
2022.70	$(1,2)^+$	384.44	$\leq$ 1
		1000.4 (3)	0.7 (3)
		1053.8 (4) d	1.1 (5)
		1148.20 (14) d	0.6 (2)
		1190.87	$\leq$ 1
		1965.22 (12) d	4.3 (4) u

a: The quoted energy is the transition energy derived from the level energies, if no error is given. Lines, which are unresolved multiplets in the singles spectrum are marked by d.

b: Gamma-ray intensity, as derived in the present work and in [2], normalized to I_γ(409 keV)=1000 (for absolute intensity per 100 decays multiply by 0.0095). The various symbols have the following meaning:

c: Intensity from $e^- - \gamma$ coincidences

f: Line masked by K X-ray

g: I_γ derived from L_I conversion line

h: I_γ derived from a comparison of the 367.1 keV and 372.6 keV lines in the coincidence spectra with lines depopulating the 1432 keV level, with α_{tot}(18.41 keV) = 6.59

m: γ-ray is masked by another line

D: γ-ray is observed by Dalmasso et al. [3]

u: undivided intensity from singles spectrum

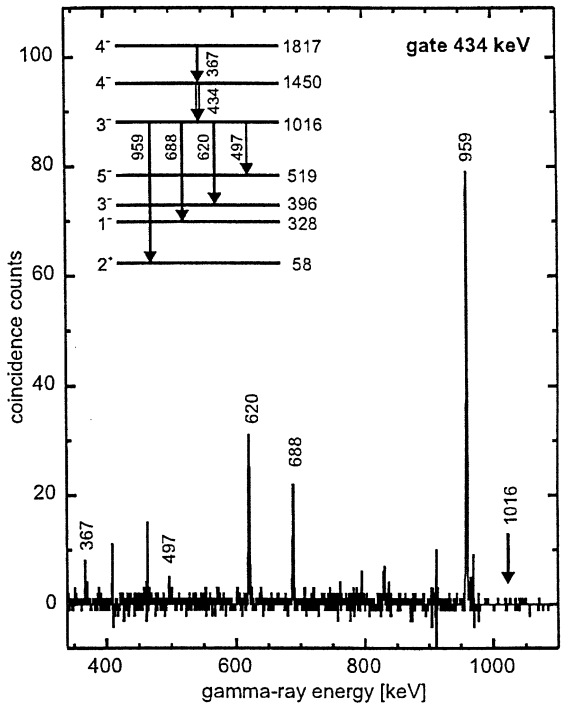

Fig. 1. Gamma-ray spectrum in coincidence with 434 keV γ-rays

2.2 $\gamma - \gamma$ coincidence spectra

In this section we will present examples of coincidence spectra to illustrate the quality of the data and to demonstrate some important new results. A further example, and perhaps the most important one for our understanding of the vibrational structure of ^{228}Th, has been given previously [4]: in the earlier work [2,3] a level was proposed at 968 keV with spin-parity of 3^-, based on the placement of transitions from this level to the 1^-, 3^- and 5^- members of the first-excited $K^\pi = 0^-$ band. From the coincidence spectra with the two strongest transitions assigned earlier as populating this level we found that it is in fact a doublet of levels separated by $\sim$ 0.1 keV, which decay to the 1^- and 3^- levels, and the 3^- and 5^- levels, respectively (see Fig. 1 of [4]). These two levels are now interpreted as 2^- and 4^+ members of the first-excited $K^\pi = 1^-$ and 0^+ bands.

The γ-ray spectrum in coincidence with a 434 keV transition is shown in Fig. 1. The 434 keV γ-ray was placed in our earlier work as transition from a 4^- level at 1450 keV to a level at 1016 keV. The spin-parity of this latter level was restricted to 2^+ or 3^-, and 2^+ was assigned to it in [3] based on the partial placement of a 1016 keV γ-ray as transition from this level to the ground state. We had adopted this assignment although it would be in question if the placement of the 434 keV γ-ray was correct. As is apparent from Fig. 1 this placement is indeed correct, but there is no evidence for the previously suggested depopulation of the 1016 keV level by a ground-state transition: from the coincidence spectrum we obtain I_γ(1016 keV)/I_γ(959 keV)$\leq 10^{-2}$ as compared to a value

Table 2. Population of levels in ^{228}Th in the EC-decay of ^{228}Pa

Level [keV]	I^π	^{228}Pa → ^{228}Th^a I[%]	log (ft)	Level [keV]	I^π	^{228}Pa → ^{228}Th^a I[%]	log (ft)
57.76	2^+	≤9.8	≥8.3	1643.15	$(2,3)^-$	1.17 (5)	7.89 (4)
186.82	4^+	2.5 (11)	8.87 (27)	1643.8	$(2,3,4)^+$	0.44 (4)	8.31 (5)
328.00	1^-	≤0.89	≥9.2	1645.92	3^+	4.10 (32)	7.34 (5)
378.17	6^+	≤0.13	≥10.0	1667.3		0.07 (2)	9.08 (12)
396.08	3^-	1.0 (5)	9.17 (31)	1678.4	$2,3,4^+$	0.44 (3)	8.24 (4)
519.20	5^-	0.22 (13)	9.76 (40)	1682.71	$2^+,3,4^+$	≤0.2	≥8.5
695.4	7^-	≤0.02	≥10.7	1683.77	(4^-)	0.35 (2)	8.32 (5)
831.83	0^+	≤0.04	≥10.4	1688.39	$(2,3)^+$	0.42 (25)	8.24 (41)
874.40	2^+	0.30 (5)	9.40 (9)	1707.2	$2,3^-$	≤0.04	≥9.2
938.6	0^+	0.025 (13)	10.42 (33)	1724.28	2^+	2.9 (2)	7.31 (4)
944.20	1^-	≤0.05	≥10.1	1735.7	$2^+,3,4^+$	≤0.09	≥8.7
968.33	2^-	0.21 (6)	9.47 (16)	1743.88	4^+	0.76 (3)	7.84 (4)
968.43	4^+	0.18 (9)	9.54 (34)	1757.9	$1^-,2,3^-$	0.043 (9)	9.05 (12)
968.97	2^+	8.6 (18)	7.85 (12)	1760.25	$(2,3)^+$	0.064 (37)	8.86 (40)
979.52	2^+	≤0.04	≥10.1	1796.4	$3^+,4,5^+$	≤0.15	≥8.3
1016.45	3^-	0.12 (7)	9.69 (41)	1802.9	$1^-,2,3^-$	0.04 (1)	8.95 (16)
1022.53	3^+	≤0.92	≥8.7	1804.60	(4^+)	1.64 (18)	7.31 (8)
1059.91	4^-	0.13 (4)	9.60 (18)	1811.5	$1^-,2,3^-$	0.090 (14)	8.55 (11)
1074.8	4^+	≤0.02	≥10.4	1817.43	4^-	0.825 (50)	7.57 (6)
1091.01	4^+	≤0.38	≥9.1	1823.4	$3^-,4,5$	0.028 (6)	9.02 (14)
1120.1	0^+	(≤0.05)	(≥ 10)	1842.2	$2^+,3^-$	0.11 (1)	8.36 (7)
1122.95	2^-	0.5 (4)	8.94 (65)	1864.8	$1^-,2,3^-$	0.39 (2)	7.72 (5)
1143.2	5^-	≤0.04	≥10.1	1876.5	$3^-,4,5^-$	0.027 (8)	8.83 (18)
1153.48	2^+	1.04 (20)	8.61 (11)	1879.0	$3^-,4,5^-$	0.031 (8)	8.75 (16)
1168.37	3^-	0.61 (26)	8.7 (2)	1892.99	3^+	4.17 (13)	6.56 (4)
1174.52	5^+	≤0.03	≥10.1	1899.98	2^+	0.57 (3)	7.38 (5)
1175.5	2^+	0.052 (25)	9.89 (30)	1901.90	4^+	0.256 (22)	7.72 (7)
1200.54	3^+	0.54 (25)	8.86 (36)	1908.4	(3^-)	0.14 (2)	7.96 (10)
1226.57	4^-	≤0.31	≥9.0	1924.1	$2^-,3,4$	0.14 (2)	7.84 (9)
1261.5	4^+	0.21 (4)	9.21 (10)	1924.6	$(4,5^+)$	0.094 (11)	8.03 (9)
1270.0	6^+	≤0.001	≥11.5	1925.20	4^+	1.79 (9)	6.75 (5)
1290.2	4^+	0.12 (4)	9.42 (18)	1928.54	3^+	0.20 (3)	7.68 (10)
1297.37	5^-	0.10 (7)	9.50 (52)	1938.9	4	0.135 (16)	7.78 (9)
1344.1	3^-	0.04 (2)	9.82 (23)	1944.88	3^+	8.1 (2)	5.96 (5)
1393.4	$1^+,2,3^-$	0.04 (2)	9.79 (30)	1945.8	$4^+,5^-$	0.18 (3)	7.61 (10)
1416.0	$2^+,3^-$	≤0.09	≥9.4	1949.7	$1^+,2,3^-$	0.09 (1)	7.89 (10)
1431.98	4^+	32.8 (13)	6.79 (4)	1958.3	(2^+)	0.062 (7)	7.98 (9)
1448.8	$3,4^-$	≤0.07	≥9.4	1964.90	(2^+)	0.125 (22)	7.61 (13)
1450.39	4^-	9.5 (6)	7.32 (5)	1974.20	4^+	0.305 (17)	7.15 (7)
1497.7	$4^+,5^-$	0.12 (2)	9.14 (7)	1981.97	$3,4^+$	0.27 (2)	7.14 (7)
1531.47	3^+	0.88 (15)	8.21 (10)	2010.14	$2^+,3$	0.23 (2)	6.92 (7)
1581.0	(2^-)	0.16 (2)	8.88 (5)	2016.75	$4^+,5^-$	0.08 (1)	7.32 (10)
1588.33	4^-	5.9 (3)	7.30 (4)	2022.70	$(1,2)^+$	0.056 (24)	7.39 (26)
1638.26	2^+	≤0.07	≥9.1				

a) I [%] is the intensity in beta-decay, as derived from the total intensities of populating and depopulating transitions between levels in ^{228}Th. The logft values are calculated with Q_{EC} = 2148 (5) keV, $T_{1/2}$(^{228}Pa; EC)= 22.4 (10) h [6] and log ($f_0^\epsilon + f_0^+$) values (as in [2])

of $6 \cdot 10^{-2}$ derived from the singles γ-ray intensities given in [3] (the 1016 keV γ-ray observed in the ^{228}Ac decay is alternatively assigned in [3] as a transition from the 1344 keV 3^- level to the 328 keV 1^- level). Spin-parity of 3^- is now established for the 1016 keV level from its population and depopulation (see the insert in Fig. 1).

A 2^+ level was proposed in [3] at 1175 keV which could not be confirmed by our earlier work. This level is now also

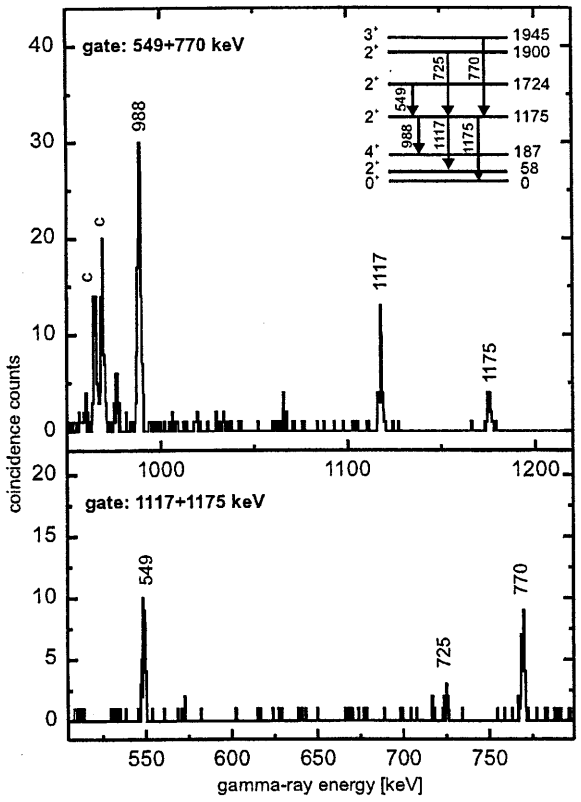

Fig. 2. $\gamma - \gamma$ coincidence spectra for the 1175 keV (2^+) level

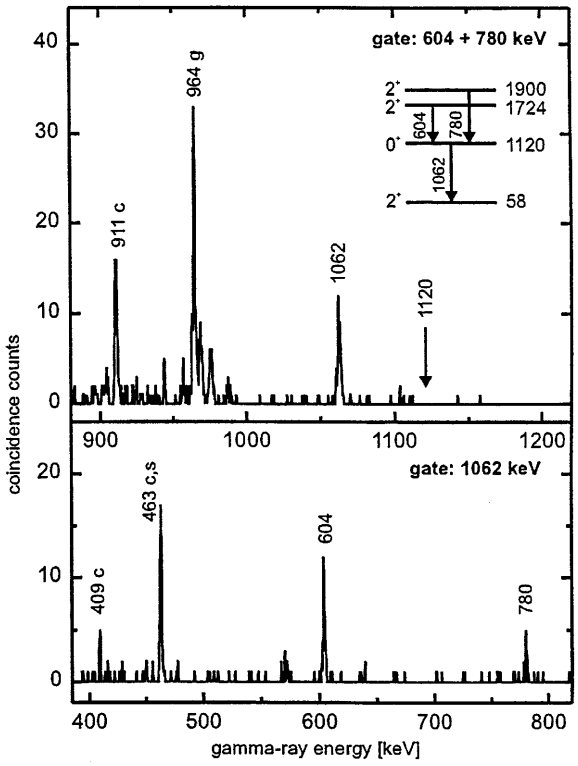

Fig. 3. $\gamma - \gamma$ coincidence spectra for the 1120 keV (0^+) level. g: coincidence with the 782 keV line (in the 780 keV gate), c: chance coincidences, s: coincidence with the 969 keV+$K_{\alpha 1}$ sum-line (in the 1062 keV gate)

observed in the ^{228}Pa decay as shown in Fig. 2. The large intensity of the 988 keV $E2$ transition from this level to the 4^+ member of the ground band excludes a $K^\pi = 2^+$ assignment. Because a $K^\pi = 1^+$ assignment is unlikely it is suggestive that this level be the 2^+ member of a $K^\pi = 0^+$ band. The corresponding 0^+ level is expected to lie around 1120 keV where we indeed observe a level with the appropriate depopulation properties as shown in Fig. 3.

Finally, we show in Fig. 4 two coincidence spectra with gate transitions used to identify a new level at 1393 keV. These spectra illustrate the sensitivity limit of our $\gamma - \gamma$ coincidences. The 1393 keV level will be tentatively assigned below as the head of a $K^\pi = 1^+$ band.

From the $\gamma - \gamma$ coincidences we assign approximately 500 γ-rays to transitions between 87 levels in ^{228}Th, from which 32 are proposed for the first time. The energies and intensities of these γ-rays are listed in Table 1. A list of the levels together with their population intensities and logft values is given in Table 2. The latter values were calculated as described in [3] with an updated value of 2148 keV for Q_{EC} [6].

2.3 $E2/M1$ mixing ratios

As mentioned above we can obtain $\gamma - \gamma$ angular correlation ratios $W(90°)/W(180°)$ from the measured $\gamma - \gamma$ concidences. These ratios could in principle restrict the spins of those levels, for which the spin-parity assignments are not established from their population and depopulation. Unfortunately, our experimental data for these levels, which are all only populated very weakly in the ^{228}Pa decay, are too inaccurate to allow safe conclusions. We can, however, use the $W(\theta)$-ratios for the determination of $E2/M1$ mixing ratios for several of the strong transitions between levels with equal parity and $|\Delta I| \leq 1$.

The $\gamma - \gamma$ angular correlation for a cascade $I_1 \rightarrow I \rightarrow I_2$ has the form

$$W(\theta) = 1 + A_{22} \cdot P_2(cos(\theta)) + A_{44} \cdot P_4(cos(\theta)) \qquad (1)$$

where the A_{kk} coefficients are the product of coefficients $A_k(\gamma_i)$ which are determined by the spins and multipolarities involved in the i′th transition. We will assume that all observed transitions have $E1$, $M1$ or $E2$ multipolarities and that only $M1 + E2$ mixtures are possible. In this case the $A_k(\gamma_i)$ have the form

$$A_k(\gamma_i) = \frac{F_k(11I_iI) + 2 \cdot \delta_i \cdot F_k(12I_iI) + \delta_i^2 \cdot F_k(22I_iI)}{1 + \delta_i^2} \qquad (2)$$

where δ_i is the $E2/M1$ mixing ratio ($\delta^2 = I_\gamma(\mathrm{E2})/I_\gamma(\mathrm{M1})$) and the F-coefficients are tabulated in the literature (see e.g. [7]).

In Fig. 5 the ratio $W(90°)/W(180°)$ is plotted for the $1^- \rightarrow 1^- \rightarrow 0^+$ and $3^- \rightarrow 3^- \rightarrow 2^+$ cascades as a function of the $E2$ content $Q = \delta^2/(1+\delta^2)$ of the first transition. A

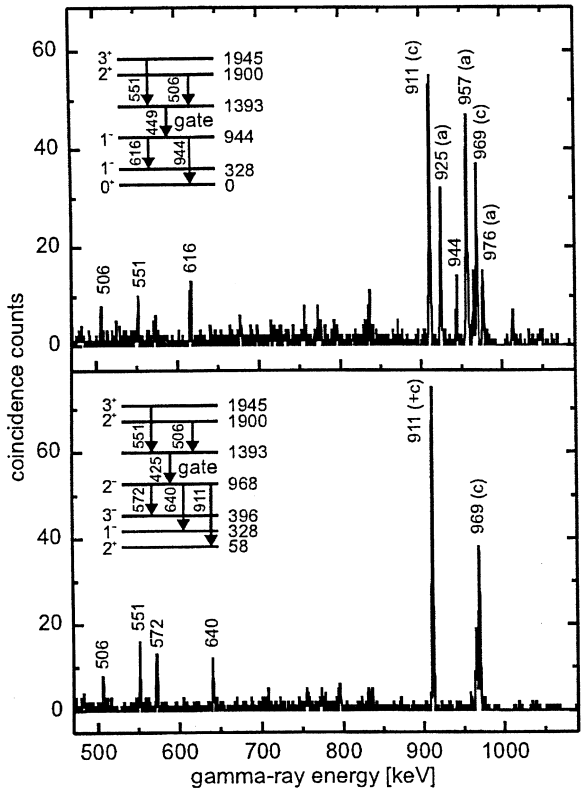

Fig. 4. $\gamma-\gamma$ coincidence spectra for the 1393 keV level. a: lines populating the 968 keV (4^+) level which is also depopulated by a 449 keV line. c: chance coincidences

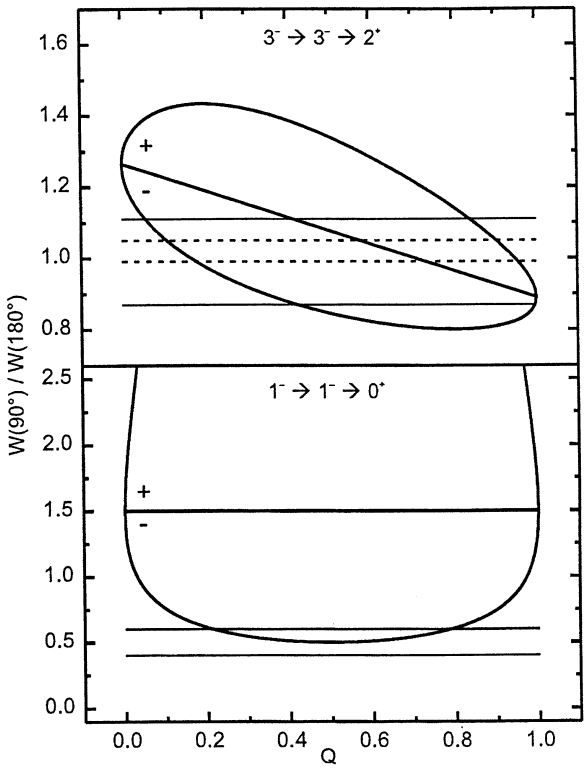

Fig. 5. Angular correlation rations $W(90^\circ)/W(180^\circ)$ for several $\gamma-\gamma$ cascades as a function of the $E2$-content Q of the first transition (see text)

particularly amazing case is the $1^- \rightarrow 1^- \rightarrow 2^+$ cascade with $A_{22} = -(1/4) \cdot (1 + 6\delta + \delta^2)/(1 + \delta^2)$ and $A_{44} = 0$, yielding the symmetrical form of $W(90°)/W(180°) = (1 - A_{22}/2)/(1 + A_{22})$ with a value of ∞ for $\delta = +1$. The experimental $W(\theta)$-ratios for the corresponding $\gamma-\gamma$ cascades from the 1^- and 3^- members of the $K^\pi = 1^-$ and 2^- bands are shown as horizontal lines in Fig. 5 (full and dashed lines, respectively).

The $E2/M1$ mixing ratios for those transitions, for which the new results are more precise than earlier values, are listed in Table 3. For comparison the earlier results [2] are also included. For the mixing ratios we have adopted the phase convention of Krane and Steffen [8] which is also used in the nuclear orientation work: the sign of δ derived from the $W(90°)/W(180°)$ ratios is reversed in Table 3, if the mixed transition is the first one in the $\gamma - \gamma$ cascade.

3 Discussion

We will devide our discussion into two parts. In a first part we present a phenomenological analysis of the excited levels, their grouping into rotational bands and their electromagnetic decay. In the second part the results of this analysis will be compared to the quasiparticle-phonon nuclear model (QPNM).

3.1 Phenomenological interpretation of the level scheme

In this section we will discuss the results of the present work which provides information beyond the published work. The organization of this section and the notations follow those of [2].

3.1.1 Octupole vibrational bands

The low-lying negative-parity excitations with $K^\pi = 0^-$, 1^-, 2^- and 3^-, which are generally interpreted as octupole vibrations, are shown in Fig. 6. We believe that this is the first case in the actinide region where all four members of the octupole quadruplet have been identified. The $K^\pi = 0^-$ and 2^- bands were established in earlier works, and the bandhead of the $K^\pi = 3^-$ band at 1344 keV was proposed in [3] and confirmed in the present work.

The structure of the $K^\pi = 1^-$ band shown in Fig. 6 is based on the new assignment of the levels at 968.3 and 1016.5 keV as the 2^- and 3^- members of this band (see sect. 2.2). The population and depopulation of these levels restrict the spin-parity of the 968 keV level to 2^- or 3^- and establish 3^- for the 1016 keV level. The previously proposed assignment of $I^\pi = 1^+$ for the 944 keV level [2], which was primarily based on its non-observation in the ^{230}Th(p,t) reaction, is excluded by the observation of a transition from this level to the 396 keV 3^- level.

Table 3. $E2/M1$ mixing ratios δ for transitions in ^{228}Th

Initial level (keV)	I^π	Final level (keV)	I^π	E_γ (keV)	δ this work	δ ref.[2]	$1/\delta^a$ this work	$\%E2$
944.2	1^-	328.0	1^-	616.2	$0.5 \leq \delta \leq 2$			$20 \leq \%E2 \leq 80$
969.0	2^+	57.8	2^+	911.2		24(8)	0.10(3)	99.0(7)
1022.5	3^+	57.8	2^+	964.8		$-7.2(10)$	0.03(4)	99.9(1)
		186.8	4^+	835.7		≤ -9	$-0.014(25)$	99.9(1)
1091.0	4^+	186.8	4^+	904.2		≥ 3.7	$-0.17(8)$	96.7(25)
1123.0	2^-	396.1	3^-	726.9			$-0.02(8)$	99.5(5)
1168.4	3^-	396.1	3^-	772.3		$-19 \leq \delta \leq -3$	$-0.27(6)$	93(3)
1226.6	4^-	396.1	3^-	830.5		$-7.7(9)$	$-0.08(3)$	99.3(5)
		519.2	5^-	707.4			$-0.25(8)$	94(4)
1297.4	5^-	519.2	5^-	778.1			$-0.33(20)$	88(10)
1450.4	4^-	1168.4	3^-	282.0	$-0.55(10)$	$-0.51(12)$		22(5)
1724.3	2^+	969.0	2^+	755.3	0.04(4)	$\lvert\delta\rvert \leq 0.6$		≤ 0.7
		1022.5	3^+	701.7	0.4(2)			15(11)
1944.9	3^+	969.0	2^+	976.0	$-0.06(5)$	0.00(5)		≤ 1.2

a) For transitions with dominant $E2$ multipolarity it is more convenient to list $1/\delta$

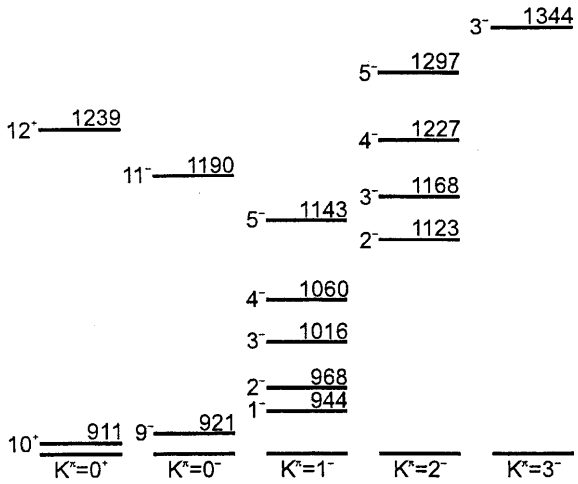

Fig. 6. One-phonon octupole-quadruplet. For the $K^\pi = 0^-$ band with its bandhead at 328 keV only the 9^- and 11^- members are shown

This leaves 1^- or 2^+ for the 944 keV level. The energies of these levels then strongly suggest that they form, together with the known 1060 keV 4^- level, the lowest members of a $K^\pi = 1^-$ band. The 5^- member of this band is suggested at 1143.2 keV, for which I^π is restricted to 4^+ or 5^- from its population and depopulation. A level at this energy is also observed in the (p,t) reaction [9] supporting this assignment. It is perhaps worthwhile to mention, that Kurcewicz et al. [1] had already proposed the 2^- and 3^- levels of the $K^\pi = 1^-$ band and only failed to identify the correct 1^- member of this band.

The octupole bands are expected to be strongly coupled by the Coriolis force, and the observation of the complete octupole quadruplet allows an analysis of this coupling. We have performed such a mixing calculation yielding a good description of the octupole bands up to the 4^- members and reasonable results for the parameters involved as discussed in [4].

It is interesting to investigate whether the known octupole bands in the neighbouring nuclei ^{230}Th and ^{232}Th can be described by the same approach for the Coriolis coupling as used in [4]. In both nuclei the $K^\pi = 0^-$, 1^- and 2^- bands are reported in the literature (see e.g. refs. [10-12]). In ^{230}Th these bands can be described using reasonable values for the parameters involved. However, the rotational bands as proposed in [12] for ^{232}Th can not be described satisfactorily. The reason for this failure can be traced to the proposed 2^- and 3^- members of the 1^- and 2^- bands. These two bands are located very close to eachother leading to a strong coupling. The experimental energy spacings of their 2^- and 3^- members proposed in [12] is 67.4 and 77.0 keV, respectively. Any reasonable coupling leads to a larger difference for these energy spacings. We note in this connection that the assignment of a 1054 keV level as bandhead of the 2^- band in [12] is questioned in [11], and that the Coriolis coupling calculation suggests a 2^- bandhead at $\sim$1072 keV. A level is observed at this energy in ^{232}Th for which, however, $I^\pi = 2^+$ is suggested in [13].

Interesting information on the transition matrix-elements for the decay of the octupole bands can be obtained from an analysis of the γ-ray branching ratios. We will discuss the results obtained for the $K^\pi = 0^-$ and 1^- bands, and refer for the 2^- and 3^- bands to the discussion given in [2].

The levels of the $K^\pi = 0^-$ band can decay by intraband $I^- \rightarrow (I-2)^-$ $E2$ transitions and by $E1$ transitions to the ground band. The $E1/E2$ γ-ray branching ratios can be interpreted in terms of intrinsic electric dipole ($\mathcal{D}_0$) and quadrupole ($\mathcal{Q}_0$) moments. For ^{228}Th the $\mathcal{D}_0/\mathcal{Q}_0$ ratios have been determined from the decay of the 9^-, 11^- and 13^- members of the 0^- band from an in-beam investigation in the ^{226}Ra$(\alpha, 2n\gamma)$ reaction [14] to have an aver-

age value of $|\mathcal{D}_0/\mathcal{Q}_0| = 1.44\,(3) \cdot 10^{-4}\,\mathrm{fm}^{-1}$. The γ-ray intensities of the $3^- \to 1^-$ and $5^- \to 3^-$ transitions are too small to be observed directly, due to their small energies (68 and 123 keV, respectively). But the total branchings of these transitions are enhanced by their large conversion coefficients, and can be derived from our measured coincidence spectra. From the γ-ray spectra in coincidence with transitions populating the 3^- and 5^- levels, we obtain intensity ratios $I_\gamma(I^- \to (I-1)^+)/I_\gamma((I-2)^- \to (I-3)^+) = 80\,(30)$ and 18 (7) respectively. From these intensity ratios the $I^- \to (I-2)^-$ γ-ray branchings can be derived using theoretical conversion coefficients for the $E1$ and $E2$ transitions involved [15], from which $|\mathcal{D}_0/\mathcal{Q}_0|$ ratios of $1.4\,(3) \cdot 10^{-4}$ fm^{-1} and $1.1\,(3) \cdot 10^{-4}$ fm^{-1} are obtained for the 3^- and 5^- levels, respectively.

In a recent in-beam investigation of $\gamma-\gamma$ coincidences in the ^{226}Ra$(\alpha, 2n\gamma)$ reaction we were able to observe the $7^- \to 5^-$ $E2$ transition and the $15^- \to 14^+$ $E1$ transition of the alternating-parity ground band in addition to the other transitions among these bands observed in our previous work [14]. For $|\mathcal{D}_0/\mathcal{Q}_0|$ we obtain results of $1.6\,(3) \cdot 10^{-4}$ fm^{-1} and $1.6\,(4) \cdot 10^{-4}$ fm^{-1} for the 7^- and 15^- levels, respectively [5]. The new results are all consistent with the previously derived average from the 9^-, 11^- and 13^- levels, proving that $\mathcal{D}_0/\mathcal{Q}_0$ is independent of spin within approximately 25% up to the 15^- level.

The $E1$ transitions from the 1^- band to the ground band are known to be strongly influenced by the $K^\pi = 0^-$ admixtures resulting from its Coriolis coupling with this latter band. If the coupling of these bands is treated in first-order perturbation theory, with mixing amplitudes of $\epsilon_0 \cdot \sqrt{2I(I+1)}$, the $B(E1)$ ratios from the $K^\pi = 0^-$ and 1^- bands can be written in the form

$$\frac{B(E1, I^-K \to (I+1)^+0)}{B(E1, I^-K \to (I-1)^+0)} = \frac{I+1-K}{I+K} \left| \frac{1+(-)^{K+1} \cdot (I+K) z_K}{1+(-)^K \cdot (I+1-K) z_K} \right|^2 \qquad (3)$$

with

$$z_0 = \sqrt{2} \cdot \epsilon_0 \cdot \frac{\langle 0_g^+ | \mathcal{M}(E1,-1) | 1_1^- \rangle}{\langle 0_g^+ | \mathcal{M}(E1,0) | 0_1^- \rangle}$$

$$z_1 = \sqrt{2} \cdot \epsilon_0 \cdot \frac{\langle 0_g^+ | \mathcal{M}(E1,0) | 0_1^- \rangle}{\langle 0_g^+ | \mathcal{M}(E1,-1) | 1_1^- \rangle}$$

The $E1$ branching from the $K^\pi = 0^-$ band yields $z_0 = -0.004\,(3)$ [2]. For the 1^- and 3^- members of the $K^\pi = 1^-$ band only the $I^- \to (I-1)^+$ transitions are observed. From the experimental intensity limits of the $I^- \to (I+1)^+$ transitions we obtain an upper limit for the $B(E1)$ ratio of 0.05 for both levels yielding $z_1 = -0.35\,(5)$.

The reduced mixing amplitude $\epsilon_0 = h_{01}/[E(K=1) - E(K=0)]$ can be obtained from the Coriolis coupling calculation described in [4] as $|\epsilon_0| = 0.026$. With this value and the experimental z_1 one obtains

$$\left| \frac{\langle 0_g^+ | \mathcal{M}(E1,-1) | 1_1^- \rangle}{\langle 0_g^+ | \mathcal{M}(E1,0) | 0_1^- \rangle} \right| = \left| \frac{\sqrt{2}\epsilon_0}{z_1} \right| = 0.105 \pm 0.022 \quad \text{and}$$

$$z_0 = 2 \cdot \epsilon_0^2 / z_1 = -0.0039 \pm 0.0013$$

where we have assumed a 15% uncertainty in ϵ_0. This value of z_0 agrees with the value obtained from the $E1$ branching ratios. With the experimental values for $|\mathcal{D}_0/\mathcal{Q}_0|$ and $\mathcal{Q}_0$ one finally obtains [2,14]

$$|\langle 0_g^+ | \mathcal{M}(E1,0) | 0_1^- \rangle| = 0.059 \pm 0.003\,\mathrm{e \cdot fm}$$
$$|\langle 0_g^+ | \mathcal{M}(E1,-1) | 1_1^- \rangle| = 0.0062 \pm 0.0013\,\mathrm{e \cdot fm}$$

The large $E1$ matrix element for the $\Delta K = 0$ transitions is usually attributed to octupole deformations. However, the results of the calculations discussed in Sec. 3.2 below show that large $E1$ transitions are obtained without explicit inclusion of such a deformation.

The levels of the $K^\pi = 1^-$ band decay, in addition to the $E1$ transitions to the ground band, by $M1 + E2$ transitions to the members of the $K^\pi = 0^-$ band. The relative γ-ray intensities are compared to the intensities expected for pure $E2$ transitions in Table 4. The most striking feature is the smallness of the γ-ray intensities for the $I \to I$ $E2$ transitions for $I \geq 3$ compared to the observed intensities (the small $E2$ branchings of the $I \to I$ transitions are due to the Clebsch Gordan coefficients involved: the $B(E2)'$s for these transitions are reduced, compared to the $I \to I \pm 2$ transitions, by factors of $6/[(2I-1)(2I+3)]$). It is quite unlikely that this is an effect of band mixings: the $E2$ branching from the 3^- level to the 1^- and 5^- levels agrees with the value for unmixed bands. For the mixing discussed in [2] with matrix elements M_1 and M_2, where M_2 causes deviations from the unperturbed mixing ratios, one obtains $|M_2/M_1| \leq 0.05$ and e.g. an increase of $B(E2, 3^- \to 3^-)$ by at most a factor of 2.

If one assumes that the additional intensity of the $I \to I$ transitions results from $M1$ transitions between the unperturbed bands one can reproduce the observed intensities reasonably well with a ratio of $E2$ to $M1$ matrix elements of

$$\left| \frac{\langle 0_1^- | \mathcal{M}(E2,-1) | 1_1^- \rangle}{\langle 0_1^- | \mathcal{M}(M1,-1) | 1_1^- \rangle} \right|^2 = (2.6 \pm 0.6) \cdot 10^4 \cdot \frac{\mathrm{e^2 fm^4}}{\mu_N^2} \quad .$$

We note that the values of $Q = \delta^2/(1+\delta^2) = 0.29$ and 0.04 for the $1^- \to 1^-$ and $3^- \to 3^-$ transitions, respectively, calculated with this ratio of $M1$ to $E2$ matrix elements, are consistent with the experimental results (see e.g. Fig. 5).

The $E2$ matrix element can be obtained from a comparison of the $I^- \to (I \pm 2)^-$ $E2$ transitions with the $E1$ transitions $I^- \to (I-1)^+$ from the 1^- and 3^- levels. Taking into account the above quoted value for z_1 in the $E1$ matrix-elements one obtains consistent results for the ratios of transition matrix-elements (the ratios derived from the 1^- and 3^- levels differ by almost a factor of two if the z_1 correction is not applied), and with the $E1$ matrix element determined above

$$|\langle 0_1^- | \mathcal{M}(M1,-1) | 1_1^- \rangle| = (0.11 \pm 0.03)\,\mu_N$$
$$|\langle 0_1^- | \mathcal{M}(E2,-1) | 1_1^- \rangle| = (18 \pm 4)\,\mathrm{e \cdot fm^2} \quad .$$

The $E2$ matrix element can be compared to the Weisskopf estimate $\sqrt{B_w(E2)} = 9.1\,\mathrm{e}\cdot\mathrm{fm}^2$ indicating an enhancement of the $K^\pi = 1^- \to K^\pi = 0^-$ transitions. This is in contrast to the calculation discussed below which predicts very small $B(E2)'$s. However, it is known that the mutual mixing of the two bands induced by the Coriolis-interaction leads to a renormalization of the $E2$ matrix elements which has in first order the form [2,16]

$$\langle 0_1^-|\mathcal{M}(E2,-1)|1_1^-\rangle \Longrightarrow$$
$$\Longrightarrow \langle 0_1^-|\mathcal{M}(E2,-1)|1_1^-\rangle - \sqrt{6}\epsilon_0\langle 0_1^-|\mathcal{M}(E2,0)|0_1^-\rangle$$

Table 4. Gamma-ray branching ratios for the transitions from the $K^\pi = 1^-$ band to the $K^\pi = 0^-$ band in ^{228}Th

Initial level		Transition			
E (keV)	I^π	$I \to I'$	E_γ(exp)	I_γ(exp)	I_γ(E2)^a
944.20	1^-	$1^- \to 1^-$	616.2	100 (7)	40.4
		$\to 3^-$	548.1^b	15 (4)	15*
968.33	2^-	$2^- \to 1^-$	640.3	100 (14)	100*
		$\to 3^-$	572.3	159 (16)	228
1016.45	3^-	$3^- \to 1^-$	688.3	59 (8)	59*
		$\to 3^-$	620.3	100 (7)	5.1
		$\to 5^-$	497.3^b	12 (3)	12.1
1059.91	4^-	$4^- \to 3^-$	663.9	100 (17)	100*
		$\to 5^-$	540.7	74 (5)	72
1143.2	5^-	$5^- \to 3^-$	747.0	64 (21)	64*
		$\to 5^-$	624.0	100 (28)	1.4
		$\to 7^-$	447.6^b		5.0

a: Calculated with
$B(E2, I_iK_i = 1 \to I_fK_f = 0) \propto \langle I_i 12 - 1|I_f 0\rangle^2$ and normalized to the transitions marked by a star
b: Transition energy calculated from level energies

With $\epsilon_0 = 0.026$ given above and assuming intrinsic quadrupole moments for the 0^- and 1^- bands equal to that of the ground band - $\langle 0_1^-|\mathcal{M}(E2,0)|0_1^-\rangle = 266\,\mathrm{e}\cdot\mathrm{fm}^2$ (see below) - one obtains for the Coriolis-induced term in the $E2$ matrix element a value of 17 e·fm^2 in agreement with the observed result.

The Coriolis coupling leads also to a modification of the intrinsic $M1$ matrix element for the $I_1 \to I_2$ transition of the form

$$\langle 0_1^-|\mathcal{M}(M1,-1)|1_1^-\rangle \Longrightarrow$$
$$\Longrightarrow \langle 0_1^-|\mathcal{M}(M1,-1)|1_1^-\rangle - \sqrt{2}\epsilon_0\langle 1_1^-|\mathcal{M}(M1,0)|1_1^-\rangle +$$
$$+ f(I_1,I_2)\sqrt{2}\epsilon_0[\langle 0_1^-|\mathcal{M}(M1,0)|0_1^-\rangle - \langle 1_1^-|\mathcal{M}(M1,0)|1_1^-\rangle]$$

with $f(I_1,I_2) = I_1+1$, 0, and $-I_1$ for $I_2 = I_1+1$, I_1, and I_1-1, respectively. Although this modification is not expected to have a dominant effect as it has for the $E2$ transitions, the different terms can have comparable magnitudes leading to sizeable changes in the $B(M1)'$s.

3.1.2 $K^\pi = 0^+$ and 2^+ bands

Three excited $K^\pi = 0^+$ bands and two $K^\pi = 2^+$ bands are observed in ^{228}Th below the threshold for two-

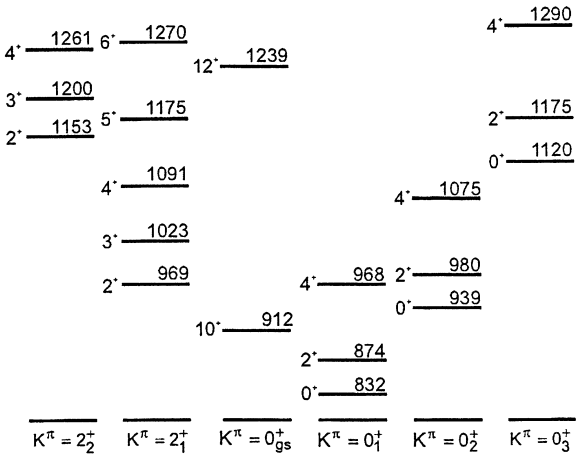

Fig. 7. $K^\pi = 0^+$ and 2^+ bands in ^{228}Th

quasiparticle excitations as shown in Fig. 7. The 0^+ and 2^+ members of the first two 0^+ bands with bandheads at 832 and 939 keV where known from previous work, although the 2^+ assignment for the 980 keV level was not unambiguously determined from experiment. This assignment is now established by the observation of the transitions to the 0^+ and 4^+ members of the ground band. The 4^+ members of these two bands are proposed at 968 and 1075 keV. These assignments are established by the depopulation of the levels: both decay predominantly to the 3^- and 5^- members of the $K^\pi = 0^-$ band and only weakly to the 2^+, 4^+ and 6^+ members of the ground band, as expected from the decay pattern of the 0^+ and 2^+ members of the two bands. The 1075 keV level is also observed in the (p,t) reaction [5,9] (the 968 keV level is masked in this reaction by the 969 keV member of the γ-band).

The third $K^\pi = 0^+$ band with its bandhead at 1120 keV is new, although all three members shown in Fig. 7 were observed in the (p,t) reaction [5,9]. The 1175 keV 2^+ member was proposed earlier in the ^{228}Ac decay [3] and is now also established in the ^{228}Pa decay (see Fig. 2). The experimental evidence for the 1120 keV 0^+ level is shown in Fig. 3. The decay of the 1290 keV level to the 4^+ and 6^+ members of the ground band is observed in the spectra in coincidence with the $4^+ \to 2^+$ and $6^+ \to 4^+$ transitions, respectively. The expected transition to the 2^+ member of the ground band could not be observed since no transitions populating the 1290 keV level were identified.

The two $K^\pi = 2^+$ bands were known up to the 5^+ and 3^+ members, respectively. The 6^+ member of the first-excited 2^+ band at 1270 keV is very weakly populated in the ^{228}Pa decay, but this level is confirmed by its observation in the ^{226}Ra$(\alpha,2n)$ reaction [17]. The 4^+ member of the second-excited 2^+ band at 1261 keV is established by a number of populating and depopulating γ-rays. Additional support comes from the observation of the 170.6 keV $4^+ \to 4^+$ $E0$ transition: in the conversion-electron spectrum we observe a previously unexplained line at $B\rho = 855$ G·cm (see Fig. 4 of [2]) which we now assign as the 170.6 keV K-conversion line. Finally we note

Table 5. Ratio of $E1$ to $E2$ transition matrix elements

Initial band E_{bh}(keV)	K_1^π	Final bands E_{bh}(keV)	K_2^π	E_{bh}(keV)	K_3^π	$\left\|\frac{\langle K_2\|\mathcal{M}(E1,K_2-K_1\|K_1\rangle}{\langle K_3\|\mathcal{M}(E2,K_3-K_1\|K_1\rangle}\right\|^a$ (fm^{-1})	
831.8	0^+	328.0	0^-	0	0^+	$(2.11 \pm 0.10) \cdot 10^{-3}$	$1.5 \cdot 10^{-3}$
938.6	0^+	328.0	0^-	0	0^+	$(2.12 \pm 0.10) \cdot 10^{-3}$	$7.4 \cdot 10^{-3}$
1120.1	0^+	328.0	0^-	0	0^+	$(0.56 \pm 0.13) \cdot 10^{-3}$	$1.2 \cdot 10^{-3}$
1123.0	2^-	969.0	2^+	328.0	0^-	$(3.72 \pm 0.09) \cdot 10^{-3}$	$3.1 \cdot 10^{-3}$
1450.4	4^-	1432.0	4^+	1123.0	2^-	$(6.9 \pm 0.6) \cdot 10^{-3}$	$17.5 \cdot 10^{-3}$

a) The numbers in the last column are the results of the QPNM calculation reported in sect. 3.2. The listed numbers can be compared to the Weisskopf estimate of $\sqrt{B_w(E1)/B_w(E2)} = 170.5 \cdot 10^{-3}$ fm^{-1}

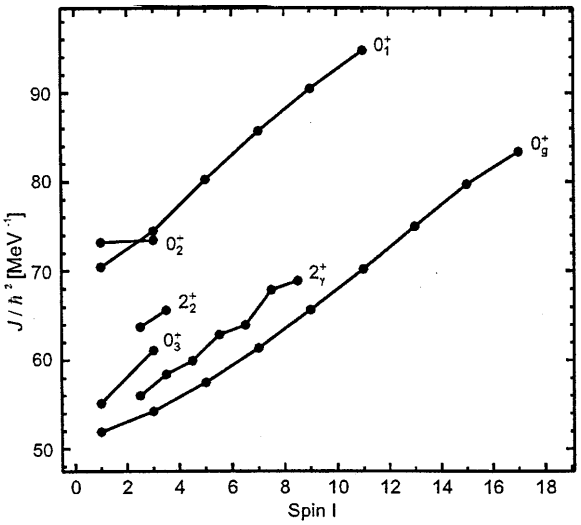

Fig. 8. Moments of inertia of the positive-parity bands in ^{228}Th

that all three members of the second-excited 2^+ band are also observed in the (p,t) reaction [5,9].

The moments of inertia for the positive-parity vibrational bands are shown in Fig. 8. The first two excited 0^+ bands have a $\sim 40\%$ larger moment of inertia than the ground band, whereas it is only 10% larger for the third 0^+ band. An analogous difference is observed for the ratios of $E1$ to $E2$ matrix elements (see Table 5) and, to some extent, also for the excitation of these levels in the (p,t) reaction. This suggests that the first two excited 0^+ bands have similar structure, whereas the third 0^+ band has a different one.

The first excited 2^+ band has a moment of inertia close to that of the ground band. This band shows all properties expected for a γ-vibration. For the second 2^+ band the moment of inertia is larger by $\sim 20\%$. In our earlier work [2] we had suggested that this latter band might be distinguished from the ground and γ-band by its shape, to explain its strong $E0$ decay to the γ-band. The observed increase of the moment of inertia is consistent with this suggestion.

The γ-ray branching ratios from the positive-parity vibrational bands have been discussed in [2]. Our new data for the $B(E\lambda)$-ratios are in accord with the previous data [5]. We will restrict our discussion to the $E2$ branching ratios where the new data allow some additional conclusions. For these discussions, as well as those of some $M1$ transitions from higher-lying levels, it is convenient to introduce the following relation for the reduced transition rates [16]:

$$B(\sigma\lambda, I_1 \to I_2) = f(I_1,I_2)|M_1 + g(I_1,I_2)\cdot M_2 + h(I_1,I_2)\cdot M_3|^2, \quad (4)$$

where the intrinsic matrix elements M_i and the spin functions f and h depend on the specific case and will be specified below for the individual cases of interest here, whereas $g(I_1,I_2)$ has the general form

$$g(I_1,I_2) = I_1(I_1+1) - I_2(I_2+1).$$

The above relation for $B(\sigma\lambda)$ with $M_3 = 0$ is termed in [16] *generalized intensity relation*.

The branching ratios of the $E2$ transitions from the γ-band to the ground band deviate appreciably from the Alaga rules as discussed in [2,17]. If one assumes that these deviations result from the coupling of the γ-band to the ground and excited 0^+-bands with coupling matrix elements of

$$\langle IK=2|H_c|IK=0\rangle = \sqrt{2(I-1)I(I+1)I+2)}\cdot h_2$$

one can express the $B(E2)'$s by relation (4) with

$$f(I_1,I_2) = 2\cdot\langle I_1 22 - 2|I_2 0\rangle^2$$
$$h(I_1,I_2) = \frac{1}{12}[(I_1(I_1+1) - I_2(I_2+1))^2 - 2(I_1(I_1+1) + I_2(I_2+1))]$$

and

$$M_1 = \langle 0_g^+|\mathcal{M}(E2,2)|2_1^+\rangle - 4\cdot M_2$$
$$M_2 = \epsilon_2\sqrt{6}\langle 2_1^+|\mathcal{M}(E2,0)|2_1^+\rangle$$
$$M_3 = \epsilon_2\sqrt{6}\left[\langle 0_g^+|\mathcal{M}(E2,0)|0_g^+\rangle - \langle 2_1^+|\mathcal{M}(E2,0)|2_1^+\rangle\right] + \sum_i \epsilon_{2,i}\sqrt{6}\langle 0_g^+|\mathcal{M}(E2,0)|0_i^+\rangle,$$

where $\epsilon_2 = h_2/[E(K=2)-E(K=0)]$ are reduced mixing amplitudes. The first term in M_3 results from different intrinsic electric quadrupole moments of the γ- and ground bands and the second term takes into account contributions resulting from the coupling of the γ-band with excited 0^+ bands (indicated by the index i). Our data can be described reasonably well with $M_2/M_1 = -0.017(4)$ (from the decay of the odd-spin levels [17]) and $M_3/M_1 = -0.015(5)$.

The $E2$ matrix elements involving the ground and γ-bands have values of

$$\langle 0_g^+|\mathcal{M}(E2,0)|0_g^+\rangle = 266 \pm 5\,\mathrm{e}\cdot\mathrm{fm}^2$$
$$\langle 2_\gamma^+|\mathcal{M}(E2,2)|0_g^+\rangle \approx 23\,\mathrm{e}\cdot\mathrm{fm}^2$$

where the second matrix element was derived from the $B(E2, 0_g^+ \rightarrow 2_\gamma^+)$ of ^{230}Th [18] including a correction for band mixing ($\delta \approx (1 + 2M_2/M_1)$ with $M_2/M_1 = -0.019$) and assuming the Grodzins relation [19]. With these values, the M_2/M_1 ratio given above and $E(K=2)-E(K=0)=$ 911 keV one obtains a spin-reduced coupling matrix element of $h_2 = -0.59\,(15)$ keV.

The matrix element M_3 results most likely from contributions of the first-excited 0^+ band, which seems to couple fairly strongly to the γ-band (see the discussion in Sec. 3.1.4) and is expected to have a large $E2$ matrix element (see e.g. [18]).

The predominant decay of the second-excited $K^\pi = 2^+$ band to the excited $K^\pi = 0^+$ bands, noted for the 1153 keV 2^+ level in [2], is confirmed for the 3^+ and 4^+ members of this band.

The three $K^\pi = 0^+$ bands decay by $E1$ and $E2$ transitions to the $K^\pi = 0^-$ and ground band, respectively. For the first two bands the $E2$ transitions from the 2^+ and 4^+ members can be analyzed using the generalized intensity relations. For the first-excited 0^+ band the $E2$ branching ratios $B(E2, I \rightarrow I+2)/B(E2, I \rightarrow I-2)$ have values of 2.1 (5) and 0.28 (10) for $I = 2$ and 4, respectively, compared to Alaga values of 2.57 and 1.59. These results can not be reproduced using the generalized intensity relation with $M_3 = 0$. If one again assumes that the deviations result from the admixtures of the γ-band to the excited 0^+ band the $B(E2)'$s can be expressed by relation (4) with

$$f(I_1, I_2) = \langle I_1 020|I_2 0\rangle^2$$
$$h(I_1, I_2) = \frac{1}{4}[(I_1(I_1+1) - I_2(I_2+1))^2 - 6(I_1(I_1+1) + I_2(I_2+1))]$$

and

$$M_1 = \langle 0_g^+|\mathcal{M}(E2,0)|0_1^+\rangle + 6\cdot M_3$$
$$M_2 = \epsilon_0\langle 0_g^+|\mathcal{M}(E2,0)|0_g^+\rangle + M_3$$
$$M_3 = -\frac{1}{3}\sqrt{6}\epsilon_2\langle 0_g^+|\mathcal{M}(E2,-2)|2_\gamma^+\rangle$$

where ϵ_0 and ϵ_2 are the reduced amplitudes of the ground and γ band, respectively, in the wave function of the 0^+ band. The experimental $E2$ branching ratios can be reproduced with $M_2/M_1 \approx 0.3$ and $M_3/M_1 \approx 0.1$. With the transition matrix elements for the ground and γ band quoted above and an estimate of ~ 21 e·fm^2 for the $0_1^+ - 0_g^+$ matrix element one would obtain $\epsilon_0 \approx 0.04$ and $\epsilon_2 \approx -0.3$. These values are too large indicating that the $E2$ transition rates from the 0_1^+ band must be influenced by additional mixing effects.

For the second-excited 0^+ band the corresponding $B(E2)$ ratios agree with the generalized intensity relation with $M_2/M_1 = -0.009\,(3)$. Although this value is not unreasonable a further analysis is not justified due to the limited data available for this band.

Consistent results are obtained for the ratios of $E1$ to $E2$ matrix elements from the decay of different members of the bands, with averages as given in Table 5.

3.1.3 Possible $K^\pi = 1^+$ band

Two additional levels are identified in ^{228}Th at 1393 and 1416 keV. Both levels are very weakly populated in the ^{228}Pa decay, and the 1416 keV level has previously also been observed in the ^{228}Ac decay. The spin-parities of these levels are restricted by their population and depopulation to $1^+, 2^\pm$ or 3^- for the 1393 keV level and 2^+ or 3^- for the 1416 keV level.

Some restriction on the spin-parity of the 1393 keV level can be obtained from the $W(90°)/W(180°)$ ratios measured for the 449-944 keV $I^\pi \rightarrow 1^- \rightarrow 0^+$ cascade. Unfortunately the statistics is poor for the 180° detectors, having only 1/4 of the weight of the 90° detectors. We observe 6 coincidence events under 180° compared to expected numbers, calculated from the 56 events observed under 90°, of 9, 13 and 15 events for $I^\pi = 1^+$, 2^+ or 3^-, and a lower limit of 10 events for $I^\pi = 2^-$ and $\delta(E2/M1) = -0.8$. This indicates that the 1393 keV level has most likely $I^\pi = 1^+$ and that the 2^+ and 3^- assignments are nearly excluded. Unfortunately, a similar analysis for the 1416 keV level is inconclusive due to the limited statistics.

If we assume that the two levels are the lowest members of a rotational band the above considerations suggest $K^\pi = 1^+$ for this band. The resulting moment of inertia of $\mathcal{J}/\hbar^2 = 88.5$ [MeV^{-1}] is rather high, but not unreasonable (see Fig. 8). Any higher K assignment would, however, lead to an unreasonable value for the moment of inertia. A level proposed at 1449 keV (see Table 1) could be the 3^+ member of this 1^+ band.

3.1.4 The 4^+ and 4^- levels at 1432 and 1450 keV

The levels at 1432 and 1450 keV are proposed below to be the vibrational states with $\lambda\mu = 44$ (hexadecapole) and $\lambda\mu = 54$. Both levels are strongly populated in the ^{228}Pa decay (and only weakly in the ^{228}Ac decay), and their spin-parity assignments are safely established. The γ-decay to the lower-lying rotational and vibrational levels

show some interesting features, which justify a separate discussion.

The 1432 keV 4^+ level decays predominantly by $E2$ transitions to the members of the γ-band. As discussed previously the $B(E2)$ ratios follow the generalized intensity relation (4) [1,2]. In addition to these strong transitions we observe weak $E2$ transitions to four lower-lying 2^+ levels. The relative $B(E2)$ values are summarized in Table 6. It is now reasonable to assume that the $E2$ transitions to the $K^\pi = 0^+$ bands result from admixtures of the γ-band to these bands and to the 4^+4 level. With coupling matrix elements for the $K^\pi = 0^+$ and 2^+ bands as given above and $\langle IK = 4|H_c|IK = 2\rangle = \sqrt{(I-3)(I-2)(I+3)(I+4)} \cdot h_4$ one obtains the relation (4) with $h(I_1, I_2)$ as given above for the $\gamma \rightarrow$ ground $B(E2)'$s and

$$
\begin{aligned}
f(I_1, I_2) &= 2(I_2-1)I_2(I_2+1)(I_2+2)\langle I_1 42-2|I_2 2\rangle^2 \\
M_1 &= \epsilon_{2,i}\langle 2_1^+|\mathcal{M}(E2,-2)|4^+\rangle + \\
&\quad + \epsilon_4 \langle 0_i^+|\mathcal{M}(E2,-2)|2_1^+\rangle - 4M_2 \\
M_2 &= -M_3 = -\sqrt{6}\cdot\epsilon_{2,i}\cdot\epsilon_4\langle 2_1^+|\mathcal{M}(E2,0)|2_1^+\rangle\,,
\end{aligned}
$$

where the different $K = 0$ bands are distinguished by the index i.

Table 6. Relative $B(E2)$ values for transitions from the 1432 keV (4^+) level to the lower-lying 2^+ levels

Final band		$B(E2, 4^+4$	$\langle K = 2_1\|h_{+2}\|K = 0_i\rangle$
E_{bh}(keV)	K^π	$\rightarrow 2^+K)^a_{rel}$	(keV)
0	0^+	$(1.4 \pm 0.4)\cdot 10^{-3}$	0.49 ± 0.07
831.8	0^+	0.100 ± 0.011	0.43 ± 0.06
938.6	0^+	0.52 ± 0.04	0.11 ± 0.01
1120.1	0^+	≤ 0.4	≤ 2
969.0	2^+	100 ± 5	
1153.5	2^+	9.1 ± 1.1	

a) Calculated from the intensities of the present work except for the 1374 keV transition, for which the intensity of [3] was used

If one assumes that the second term in M_1 is negligible, the $B(E2)$ values from the 4^+ level to the 2^+ levels are equal to $48 \cdot \epsilon_{2,i}^2 \cdot B(E2, 4^+4 \rightarrow 2^+2)$, allowing to determine the spin-reduced interaction strength $h_{2,i}$, as given in the last column of Table 6 ($h_{2,i} = \epsilon_{2,i} \cdot (E(K = 2) - E(K = 0_i))$). The strength for the coupling of the ground and γ-bands is in agreement with the value derived from the $B(E2)$ ratios of the transitions from the γ-band to the ground band indicating that the second term in M_1 is indeed small, even for the ground band where the $E2$ matrix element is large.

The 1450 keV 4^- level decays predominantly to the $K^\pi = 2^-$ band. In contrast to the 4^+ level, however, these transitions have appreciable $M1$ contents (see Tables 3 of the present work and of [2]). The $B(E2)$ ratios derived from these data deviate strongly from the Alaga rules. It is suggestive that these deviations result from admixtures of the $K^\pi = 3^-$ band to the 2^- and 4^- bands. This leads again to relation (4) with $f(I_1, I_2) = \langle I_1 42-2|I_2 2\rangle^2$, $h(I_1, I_2)$ as given above for the $\gamma \rightarrow$ground $B(E2)'$s and

$$
\begin{aligned}
M_1 &= \langle 2^-|\mathcal{M}(E2,-2)|4^-\rangle - \tilde{\epsilon_4}\langle 2^-|\mathcal{M}(E2,-1)|3^-\rangle \\
&\quad -\tilde{\epsilon_2}\langle 3^-|\mathcal{M}(E2,-1)|4^-\rangle - 12M_2 - 9M_3 \\
M_2 &= (-\tilde{\epsilon_4}\langle 2^-|\mathcal{M}(E2,-1)|3^-\rangle + \tilde{\epsilon_2}\langle 3^-|\mathcal{M}(E2,-1)|4^-\rangle \\
&\quad -3M_3)/2 \\
M_3 &= -\sqrt{6}\tilde{\epsilon_2}\tilde{\epsilon_4}\langle 3^-|\mathcal{M}(E2,0)|3^-\rangle
\end{aligned}
$$

The experimental $B(E2)$ ratios can then be reproduced almost exactly with $M_2/M_1 = -0.212$ and $M_3/M_1 = 0.245$. This indicates that all terms involved in the M_i are of comparable magnitude, and thus in particular the leading-order matrix element $\langle 2^-|\mathcal{M}(E2,-2)|4^-\rangle$ must be small.

From the $E2/M1$ mixing ratios of the transitions from the $4^\pm$ levels to the $3^\pm$ levels of the $K = 2$ bands one obtains ratios of $B(M1, 4 \rightarrow 3)/B(E2, 4 \rightarrow 3)$ of $(2.3 \pm 0.5)\cdot 10^{-5}$ W.u. and $(0.9 \pm 0.3)\cdot 10^{-3}$ W.u. for the 4^+ and 4^- band, respectively, indicating that the $B(M1)'$s are highly hindered as expected for K-forbidden transitions.

Finally, we observe indirectly the $4^- \rightarrow 4^+ E1$ transition, from which we obtain the ratio of $E1$ to $E2$ matrix elements given in Table 5.

3.1.5 Levels above 1.5 MeV

A total of 47 levels were identified above 1.5 MeV from which 21 are observed for the first time. Unfortunately, we are not able to arrange these levels into rotational bands, due perhaps partly to the limited knowledge of the spin-parities. We will therefore restrict the discussion to a few levels, for which reasonably reliable information on spin-parities is available. In Table 7 the levels are listed for which K quantum numbers could be assigned. These assignments are based on the following considerations:

Both ^{228}Ac and ^{228}Pa have $I^\pi K = 3^+3$, and therefore levels in ^{228}Th with spins and K quantum numbers of 2, 3 and 4 can be assumed to be populated by allowed Gamow-Teller (positive-parity levels) or first-forbidden (negative-parity levels) transitions. The ft values of the members of rotational bands with IK are then expected to be proportional to $1/\langle 331(K-3)|IK\rangle^2$ (see e.g. the discussion in [20]) yielding

$$
\begin{aligned}
ft(33 \rightarrow 42) : ft(33 \rightarrow 32) &: ft(33 \rightarrow 22) = 20 : 20/7 : 1 \\
ft(33 \rightarrow 43) &: ft(33 \rightarrow 33) = 3 : 1
\end{aligned}
$$

Thus, for any strongly populated 3^+ level with $K = 2$ a lower-lying 2^+ level should also be strongly populated with an even smaller logft value (log$ft(2^+)$=log$ft(3^+)-0.46$). Such 2^+ levels are not observed for the 3^+ levels at 1531, 1646, 1893 and 1945 keV, to which we therefore assign $K = 3$. A similar consideration for the 4^+ levels leads to a

Table 7. Spin-parities, K values and logft values for levels in ^{228}Th above 1.5 MeV

E_{exc}(keV)	$I^\pi K^{a)}$	log(ft)	
		^{228}Pa→ ^{228}Th	^{228}Ac→ ^{228}Th^{b}
1432.0	4^+4	6.79 *4*	8.2 *2*
1531.5	3^+3	8.21 *10*	6.96 *2*
1638.3	2^+2	$\geq$ 9.1	7.52 *2*
1643.8	4^+4?	8.31 *5*	
1645.9	3^+3	7.34 *5*	6.94 *2*
1688.4	3^+3?	8.2 *4*	7.04 *3*
1724.3	2^+1?	7.31 *4*	7.12 *2*
1743.9	4^+4?	7.84 *4*	7.65 *2*
1760.3	3^+1?	8.9 *4*	8.10 *4*
1893.0	3^+3	6.56 *4*	7.51 *4*
1900.0	2^+2?	7.38 *5*	7.66 *4*
1901.9	4^+3?	7.72 *7*	
1925.2	4^+4	6.75 *5*	
1944.9	3^+3	5.96 *5*	6.83 *4*
1974.2	4^+3?	7.15 *7*	
1450.4	4^-4	7.32 *5*	8.28 *6*
1588.3	4^-4	7.30 *4*	
1817.4	4^-4	7.57 *6*	

a) Tentative assignments are indicated by a question mark
b) from [6]

$K = 4$ assignment for the 1432 and 1925 keV levels. The 1744 and 1974 keV 4^+ levels have logft values consistent with their interpretation as rotational levels with the 1646 and 1893 keV 3^+ levels as bandheads, respectively. However, the energy differences make these assignments - at least for the 1646/1744 keV levels - questionable. Finally, the 1450, 1588 and 1817 keV 4^- levels must have $K = 4$ because of the absence of any 3^- levels with log$ft \leq 7.8$ below 1.85 MeV.

For the 2^+ levels the ratio $\frac{B(E2,2^+\to 4^+_g)}{B(E2,2^+\to 0^+_g)}$ has values of 18/7, 8/7 and 1/14 for $K = 0$, 1 and 2, respectively. The experimental $B(E2)$ ratios of 0.04 (1) and 2.6 (4) for the 1638 and 1724 keV levels, respectively, establish $K = 2$ for the former level and exclude this assignment for the latter one. A $K = 0$ assignment is suggested from the $B(E2)$ ratio for the 1724 keV level, but this would make it difficult to understand its strong $M1$ decay to the 2^+ member of the γ-band and its low logft value. We have therefore tentatively adopted $K = 1$ for the 1724 keV level in Table 7. Finally, for the 1688 and 1760 keV levels a 2^+ assignment would lead to $\frac{B(E2,2^+\to 4^+_g)}{B(E2,2^+\to 0^+_g)} \geq 10$ and ≥ 9, respectively, which would be difficult to explain.

In the following we will discuss some striking decay patterns for individual levels which might give hints on their structure. One characterictic feature of several levels discussed below is their predominant decay by $E2/M1$ transitions to the lower-lying collective levels. This suggests a comparison of the mixing ratios with $|\delta_w(E2/M1)| = 0.0566 \cdot \mathrm{E}_\gamma(\mathrm{MeV})$ derived with the Weisskopf estimates for $B(M1)$ and $B(E2)$. Since $B(E2)$ is usually enhanced for collective transitions one can view the occurance of mixing ratios comparable with δ_w as indication for non-collective excitations.

1531.5 keV level: This level is the first excited level with $K^\pi = 3^+$. It decays most strongly by an $M1$ transition to the 1432 keV 4^+ level, with a ratio of reduced transition rates for the K-allowed $M1$ transitions to the 4^+ and 2^+_γ levels of $B(M1, 3^+ \to 4^+)/B(M1, 3^+ \to 2^+) \approx 10^3$. This might indicate a structural relationship between the 3^+ and 4^+ levels.

1643.8 keV level: The populating and depopulating transitions restrict the spin-parity of this level to 2^+, $3^\pm$ or 4^+. The 3^- assignment is excluded by the ratio $\frac{W(90^\circ)}{W(180^\circ)} = 0.78\,(10)$ observed for the I^π(675 keV)2^+(969 keV)0^+ cascade. The 1643.8 keV level decays predominantly to the 2^+, 3^+ and 4^+ members of the γ-band with intensity ratios consistent with pure $E2$ transitions from a $I^\pi K = 4^+4$ level.

1688.4 keV level: As discussed above the absence of the transition from this level to the ground state suggests $I^\pi = 3^+$. The small logft value in the ^{228}Ac decay would then require $K = 3$ for this level. With the assumption of $I^\pi = 3^+$ we can derive the $E2/M1$ mixing ratio for the dominating 1631 keV transition to the 2^+_g state from the nuclear orientation measurement [2] yielding $\delta = 0.23\,(3)$ or $1/\delta = -0.02\,(3)$, compared to $|\delta_w(1631\ \mathrm{keV})| = 0.09$.

1724.3 keV level: The most striking feature of this level is its predominant decay to the 2^+_γ level, and its fairly strong decay to the 2^+_g level, both essentially pure $M1$ transitions (see Tables 3 of the present work and [2]) with $B(M1, 2^+ \to 2^+_\gamma)/B(M1, 2^+ \to 2^+_g) = 62\,(4)$. This suggests the $K = 1$ assignment given in Table 7.

1743.9 keV level: This level could be assigned as the 4^+ member of a $K = 3$ band with the 1688 keV level as bandhead. This interpretation is consistent with the energies of the two levels and their population in the ^{228}Ac decay, but inconsistent with the logft values observed in the ^{228}Pa decay and we therefore tentatively assign $K = 4$ to the 1744 keV level. One remarkable feature of this level is its proposed $E3$ decay to the 1^- member of the 0^- octupole band with

$$\frac{B(E3, 4^+ \to 1^-)}{B(E2, 4^+ \to 2^+)} = (9.2 \pm 2.1) \cdot 10^3 \cdot \frac{B_w(E3)}{B_w(E2)}.$$

This would indicate that the $E2$ transitions to the ground band are highly hindered, or that the 1744 keV level is a doublet. We should, however, emphasize that the placement of the 1365 and 1416 keV γ-rays as transitions from a level at 1744 keV to the 6^+ and 1^- levels, respectively, are safely established by the $\gamma - \gamma$ coincidences.

1760.3 keV level: For this level we had reported in [2] allowed spin-parities of 2^+, 3^+ and 3^-. However, the intensities of the γ-rays depopulating this level observed in coincidence with 185 keV K conversion-electrons [2] establish predominant $M1$ multipolarity for the 1945 keV → 1760 keV transition and thus exclude the 3^- assignment, and the absence of the transition from this level to the ground state makes 2^+ unlikely, leaving $I^\pi = 3^+$.

In this case we can derive the $E2/M1$ mixing ratio of the 1703 keV transition to the 2^+_g state from the nuclear orientation measurement [21] as $\delta = 0.22\,(8)$ or $1/\delta = -0.02\,(6)$.

From its energy and logft values the 1760 keV level could be the 3^+ member of a $K = 1$ band with the 1724 keV level as 2^+ member. The solution of almost pure $M1$ multipolarity for the 1703 keV transition would be consistent with the corresponding $M1$ decay of the 1724 keV level. Further support for this assignment comes from the decay of the 1945 keV 3^+ level to the 1724 and 1760 keV levels: assuming for both the 220 and 185 keV transitions $M1$ multipolarity (as experimentally established for the latter transition) one obtains $\frac{B(M1,3^+\to 3^+)}{B(M1,3^+\to 2^+)} = 0.62\,(6)$ close to the value of 7/8 calculated with the leading-order intensity relation for K-forbidden $M1$ transitions (eq. (4-95) of [16]).

1893.0 keV level: This level, for which $I^\pi K = 3^+3$ is strongly suggested by its logft in the ^{228}Pa decay, shows a quite unexpected γ-decay: the strongest depopulating transition is a $M1$ transition to the 3^+ member of the γ-band, whereas the transitions to the 2^+ and 4^+ members of this band are very weak. This pattern can be understood by band mixings, e.g. the mutual mixing of the two bands by the Coriolis coupling. The $B(M1)'$s are then represented by the relation (4) with

$$f(I_1, I_2) = \langle I_1 31 - 1 | I_2 2\rangle^2$$
$$h(I_1, I_2) = (-)^{I_1 - I_2} \cdot I_1(I_1 + 1)$$

and

$$M_1 = \langle 2^+_1|\mathcal{M}(M1,-1)|3^+\rangle - \sqrt{2}\epsilon\langle 2^+_1|\mathcal{M}(M1,0)|2^+_1\rangle \\ -6M_2 + 12M_3$$
$$M_2 = \sqrt{2}\epsilon[\langle 3^+|\mathcal{M}(M1,0)|3^+\rangle - \langle 2^+_1|\mathcal{M}(M1,0)|2^+_1\rangle]/2 \\ +3M_3$$
$$M_3 = \epsilon^2\langle 3^+|\mathcal{M}(M1,1)|2^+_1\rangle$$

where ϵ is the spin-reduced mixing amplitude. Assuming that all three transitions from the 3^+ level to the γ-band have $M1$ multipolarity, the γ-ray branchings can be reproduced e.g. with $M_2/M_1 = -0.010(4)$ and $M_3/M_1 = 0.055(1)$, which are not unreasonable results.

The second strongest transition depopulating the 1893 keV level is the 1835 keV transition to the 2^+_g level with $\delta = 2.9\,(3)$ [2] compared to $|\delta_w| = 0.10$. This indicates a retardation of the K-forbidden $M1$ transition which is also indicated by the ratio

$$\frac{B(M1, 3^+ \to 2^+_g)}{B(M1, 3^+ \to 3^+_\gamma)} = (7.2 \pm 1.4) \cdot 10^{-3}.$$

Finally, the value

$$\frac{B(E2, 3^+ \to 2^+_g)}{B(M1, 3^+ \to 3^+_\gamma)} = (5.4 \pm 0.4) \cdot \frac{B_w(E2)}{B_w(M1)}$$

is not inconsistent with an allowed $M1$ and an $E2$ with K forbiddenness 1.

1900.0 keV level: The 2^+ assignment for this level is established from its decay to 0^+, 3^+ and 3^- levels. It decays predominantly by a mixed $M1/E2$ transition to the 2^+ member of the ground band with δ(1842 keV, $2^+ \to 2^+$)$= -0.84\,(14)$ [2] compared to $|\delta_w| = 0.10$. The branching ratios have values of

$$B(E2, 2^+ \to 4^+_g) \ : \ B(E2, 2^+ \to 2^+_g) : B(E2, 2^+ \to 0^+_g) \\ = \leq 0.6 : (3.2 \pm 0.8) : 1.$$

If we assume that these branching ratios follow the generalized intensity relation with matrix elements M_1 and M_2 the experimental values are only consistent with $K = 2$.

1925.2 keV level: This level decays most strongly to the 4^+ member of the ground band, but no transition is observed to the 2^+_g level (I_γ(1867 keV)≤ 6). This might suggest an $I^\pi = 5^-$ assignment which is, however, excluded by the anisotropy of the 1738.5 keV γ-ray observed in the nuclear orientation measurement [2,21]. The observation of the 1547 keV transition to the 6^+_g level establishes $I^\pi = 4^+$ for the 1925 keV level, and with this assignment we obtain $0.1 \leq \delta$(1739 keV)≤ 0.8 from the nuclear orientation measurement [21]. The predominant $M1$ transition to the 4^+_g level has K forbiddenness of 3 suggesting that the 1925 keV level has considerable admixtures of lower K.

1944.9 keV level: This level is populated in the ^{228}Pa decay with the lowest logft. It decays predominantly by K-allowed $M1$ and $E1$ transitions to the γ and $K^\pi = 2^-$ band, respectively, and by K-forbidden $E2$ transitions to the ground band. The $M1$ decay to the γ-band is similar to that of the 1893 keV level, with the strongest transition to the 2^+_γ level. Assuming again for all three observed transions $M1$ multipolarity one can reproduce the branching ratios with the intensity relation given for the 1893 keV level with e.g. $M_2/M_1 = -0.03(2)$ and $M_3/M_1 = -0.018(3)$. The branchings of the $E1$ and $E2$ transitions to the 2^- and ground band can also be reproduced with the generalized intensity relations. Finally, the ratio

$$\frac{B(E2, 3^+ \to 2^+_g)}{B(M1, 3^+ \to 2^+_\gamma)} = (23 \pm 2) \cdot \frac{B_w(E2)}{B_w(M1)}$$

is comparable to the corresponding ratio observed for the 1893 keV level. There is thus a striking similarity between the 1893 and 1945 keV levels.

1901.9 and 1974.2 keV levels: These levels decay predominantly to the 3^- and 5^- members of the 0^- octupole band with $B(E1, 4^+ \to 3^-)/B(E1, 4^+ \to 5^-) = 0.77\,(10)$ and $0.90\,(11)$, respectively. The theoretical values in leading order are 4/5 for $K = 0$ and 5/4 for $K = 1, 2, 3$ and 4. This might indicate that the two levels contain appreciable $K = 0$ components, which is not inconsistent with their decay to the ground band.

1588.3 and 1817.4 keV levels: These levels decay most strongly by K allowed $M1$ transitions to the 1450 keV 4^- level. The 1588 keV level decays in addition by strong K allowed $E1$ and $E2$ transitions to the 4^+ and 3^+ levels at 1432 and 1531 keV and the 2^- and 3^- members of the

$K^\pi = 2^-$ octupole band, with ratios of reduced transition rates of

$$\frac{B(E1,4^- \to 3^+)}{B(E1,4^- \to 4^+)} = 16.2 \pm 1.1$$
$$\frac{B(M1,4^- \to 4^-)}{B(E1,4^- \to 4^+)} = (858 \pm 61) \cdot \frac{B_w(M1)}{B_w(E1)}$$
$$\frac{B(E2,4^- \to 2^-)}{B(M1,4^- \to 4^-)} = (6.8 \pm 1.2) \cdot \frac{B_w(E2)}{B_w(M1)}.$$

The 1817 keV level decays also by fairly strong transitions to the 3^- and 5^- members of the $K^\pi = 0^-$ band. Assuming 80% $E2$ multipolarity for these transitions [2] one obtains

$$\frac{B(E2,4^- \to 3^-)}{B(E2,4^- \to 5^-)} = 1.8 \pm 0.2 \quad \text{and}$$
$$\frac{B(E2,4^- \to 3^-)}{B(M1,4^- \to 4^-)} = (1.1 \pm 0.2) \cdot \frac{B_w(E2)}{B_w(M1)}.$$

The $B(E2)$ ratio agrees with the value of 2 calculated with the leading-order intensity relation for K forbidden transitions, and both branching ratios indicate again considerable admixtures of lower K for the 1817 keV level.

3.2 Comparison with the quasiparticle-phonon nuclear model

3.2.1 Description of vibrational states in the QPNM

The quasiparticle-phonon nuclear model (QPNM) [22,23] is used for a microscopic description of low-spin small-amplitude vibrational states in spherical nuclei not far from closed shells and in well-deformed nuclei. The QPNM Hamiltonian contains an average field of neutron and proton systems as a deformed axially-symmetric Woods-Saxon potential, short-range monopole and quadrupole pairing and long-range particle-hole (ph) and particle-particle (pp) isoscalar and isovector multipole and spin-multipole residual interactions.

The Hamiltonian is expressed in terms of quasiparticles by performing the Bogoliubov transformation

$$a_{q\sigma} = u_q \alpha_{q\sigma} + \sigma v_q \alpha^+_{q-\sigma} \tag{5}$$

where the $\alpha^+_{q\sigma}$ and $\alpha_{q\sigma}$ are creation and annihilation operators of quasiparticles. The quantum numbers $q\sigma$ specify the single-particle states: $\sigma = \pm 1$ characterizes the symmetry with respect to time reversal and q stands for K^π and the Nilsson asymptotic quantum numbers $Nn_z\Lambda\uparrow$ $(K = \Lambda + 1/2)$ or $Nn_z\Lambda\downarrow$ $(K = \Lambda - 1/2)$.

The one-phonon states of a doubly even nucleus are then desribed within the random-phase approximation (RPA) by wave functions

$$Q^+_{\lambda\mu i\sigma}\Psi_0 \tag{6}$$

where Ψ_0 is the ground-state wave-function of the doubly even nucleus which is considered as a phonon vacuum, and the RPA phonon operators $Q^+_{\lambda\mu i\sigma}$ have the form

$$Q^+_{\lambda\mu i\sigma} = \frac{1}{2}\sum_{q_1 q_2}\{\psi^{\lambda\mu i}_{q_1 q_2} A^+(q_1 q_2;\mu\sigma) - \phi^{\lambda\mu i}_{q_1 q_2} A(q_1 q_2;\mu{-}\sigma)\} \tag{7}$$

The operators $A^+(q_1q_2;\mu\sigma)$ and $A(q_1q_2;\mu{-}\sigma)$ are pairs of the creation and annihilation quasiparticle operators and $i = 1, 2, 3, \ldots$ is the root of the RPA secular equation. The normalization condition of the one-phonon wave function has the form

$$\frac{1}{2}(1+\delta_{\mu 0})\sum_{q_1 q_2}\left[(\psi^{\lambda\mu i}_{q_1 q_2})^2 - (\phi^{\lambda\mu i}_{q_1 q_2})^2\right] = 1 \tag{8}$$

In the QPNM one-phonon states, denoted by $(\lambda\mu)_i$, are used as a basis. A two-quasiparticle state is treated as a specific case of a one-phonon state when the root of the RPA secular equation is close to the relevant pole. The one-phonon states are calculated using the following interactions: monopole and quadrupole pairing plus ph and pp isoscalar and isovector quadrupole interactions for $K^\pi = 0^+$ states; ph and pp isoscalar and isovector quadrupole and spin-spin interactions with approximate exclusion of the spurious state for $K^\pi = 1^+$ states; ph and pp isoscalar and isovector octupole and ph isovector dipole interactions for $K^\pi = 0^-$ and 1^- states; ph and pp isoscalar and isovector interactions for all other phonons. The relevant RPA equations are given in [22-26].

The QPNM wave function consists of one- and two-phonon terms and has the form

$$\Psi_n(K^{\pi_0}_0\sigma) = \Bigg\{\sum_{i_0} R^n_{i_0} Q^+_{g_0\sigma_0} + \sum_{\substack{g_1\sigma_1\\ g_2\sigma_2}} \frac{(1+\delta_{g_1,g_2})^{1/2}\delta_{\sigma_1\mu_1+\sigma_2\mu_2,\sigma_0 K_0}}{2[1+\delta_{K_0,0}(1-\delta_{\mu_1,0})]^{1/2}} \times P^n_{g_1,g_2} Q^+_{g_1\sigma_1} Q^+_{g_2\sigma_2}\Bigg\}\Psi_0 \tag{9}$$

where $g_k \equiv \lambda_k\mu_k i_k$ and $\mu_0 \equiv K_0$. The normalization condition is

$$\sum_{i_0}(R^n_{i_0})^2 + \sum_{g_1\geq g_2}(P^n_{g_1,g_2})^2(1+\mathcal{K}^{K_0}(g_1,g_2)) = 1. \tag{10}$$

The function $\mathcal{K}^{K_0}(g_1,g_2)$ is responsible for the effect of the Pauli principle in two-phonon terms of the wave function (9). The secular equations for energies E_n have the form

$$\det||(\omega_{g_0} - E_n)\delta_{i_0 i'_0} - \sum_{g_1\geq g_2}\frac{1+\mathcal{K}^{K_0}(g_1,g_2)}{(1+\delta_{\lambda_1\lambda_2}\delta_{\mu_1\mu_2}\delta_{i_1 i_2})(1+\delta_{K_0 0}(1-\delta_{\mu_1 0}))} \times \frac{U^{g_0}_{g_1,g_2}U^{g'_0}_{g_1,g_2}}{\omega_{g_1}+\omega_{g_2}+\Delta\omega(g_1,g_2)+\Delta(g_1,g_2)-E_n}|| = 0. \tag{11}$$

Here ω_g are the RPA energies, the function $U^{g_0}_{g_1,g_2}$ is responsible for coupling of one- and two-phonon terms in (9), $g'_0 = \lambda_0\mu_0 i'_0$, $\Delta\omega(g_1, g_2)$ is the shift of the two-phonon pole due to the Pauli principle and $\Delta(g_1, g_2)$ represents the effect of the three-phonon terms added to the wave function (9).

3.2.2 Details of the calculation

The calculations were performed with the Woods-Saxon potential for $A = 229$ at equilibrium deformations of $\beta_2 = 0.19$, $\beta_4 = 0.10$ and $\gamma = 0$. The isoscalar constants $\kappa_0^{\lambda\mu}$ of the ph multipole interactions are fixed to reproduce the experimental energies of the first-excited K^π nonrotational states (except for the $K^\pi = 0^-_1$ state, as discussed below). The numerical values (in units of fm^{2}MeV^{-1}) are:

$$\begin{array}{llll} \kappa_0^{20} = 0.015 & \kappa_0^{21} = 0.016 & \kappa_0^{22} = 0.014 & \\ \kappa_0^{30} = 0.0128 & \kappa_0^{31} = 0.0113 & \kappa_0^{32} = 0.013 & \kappa_0^{33} = 0.016 \\ \kappa_0^{43} = 0.019 & \kappa_0^{44} = 0.020 & \kappa_0^{54} = 0.020 & \end{array}$$

The energy of the root of the RPA seqular equation equals zero at $(\kappa_0^{21})_{cr} = 0.015\,\mathrm{fm^2MeV^{-1}}$. In this case the spurious state is excluded approximately.

The remaining constants were chosen as follows: isovector constants $\kappa_1^{\lambda\mu} = -1.2\kappa_0^{\lambda\mu}$ for the ph interactions, the constants $G^{\lambda\mu} = 0.8\,\kappa_0^{\lambda\mu}$ for the pp interactions and $\kappa_1^{1\mu} = -1.2\kappa_0^{3\mu}$ for the isovector dipole interaction (the GDR is correctly described with these constants). The constants of the isoscalar and isovector spin-spin interactions were taken as $\kappa_0^{011} = -0.0024$ and $\kappa_1^{011} = -0.024$. Finally, the monopole pairing constants were fixed by pairing energies at $G^{20} = 0.8\,\kappa_0^{20}$. The constants used in the present work are close to those used in the earlier calculation for ^{238}U [27] except for κ_0^{30} and κ_0^{31}.

Our phonon basis consists of ten phonons ($i = 1, \ldots, 10$) for each of the multipolarities $\lambda\mu = 20, 21, 22, 30, 31, 32, 33, 43, 44$ and 54. The calculations are performed with the radial dependence of the multipole interaction in the form of $\partial V(r)/\partial r$, where $V(r)$ is the central part of the Woods-Saxon potential. The energies of the two-quasiparticle poles were calculated taking into account the blocking effect and the Gallagher-Moszkowski correction [28].

We have calculated the energies and wave functions of nonrotational states of ^{228}Th, the reduced probabilities of $E\lambda$ and $M\lambda$ transitions between these states and the ft values for the β-decay of ^{228}Ac and ^{228}Pa to ^{228}Th. The reduced transition probabilities between excited states are given by eqs. (24) and (25) in [24]. The $B(E\lambda)$ values for $\lambda = 2, 3, 4$ and 5 were evaluated with effective charges of $e^{(\lambda)}_{\mathrm{eff}}(p) = 1.2$ and $e^{(\lambda)}_{\mathrm{eff}}(n) = 0.2$ to account for the truncated space of single-particle states used in the calculation.

For the $E1$ transitions a special treatment is necessary. It has been shown in [26] that the inclusion of the isovector ph electric dipole interaction decreases the $E1$ strength in the low-energy region by more than an order of magnitude. Nevertheless, the calculated $B(E1)$ values for the excitation of the $K^\pi = 0^-$ states are 3 to 10 times larger than the experimental values. Therefore, we have used the following renormalized effective $E1$ charges

$$e^{(1)}_{\mathrm{eff}} = -\frac{e}{2}(\tau_z - \frac{N-Z}{A})(1+\chi).$$

The parameter χ is introduced to quench too strong $E1$ transitions. We calculated the reduced $E1$ transition probabilities in ^{168}Er within the QPNM and fixed $(1+\chi)^2 = 0.2$ by an overall fit of the experimental summed $E1$ strength in the energy range from 1.7 to 4.0 MeV [29]. This value was adopted in the present work for ^{228}Th. Finally, the $M1$ strength was computed by using a spin quenching factor of $g_s = 0.7$.

The β-decay matrix elements from the two-quasiparticle state of ^{228}Ac and ^{228}Pa with $K = K_\nu + K_\pi$ and the wave function $\frac{1}{\sqrt{2}}(\alpha^+_{s_{1+}}\alpha^+_{r_{2+}} + \alpha^+_{s_{1-}}\alpha^+_{r_{2-}})\Psi_0$ to the one-phonon $Q^+_{\lambda\mu i\sigma}\Psi_0$ states of ^{228}Th were calculated using eqs. (9.32′) and (9.32′′′) of [20].

The QPNM calculations are most successful in nuclei with small ground state correlations. These correlations increase with the collectivity of the first one-phonon states. The pp interaction reduces the ground state correlations and thus improves the applicability of the RPA. The number of quasiparticles with quantum number q in the ground state is

$$n_q = \sum_{\lambda\mu} n_q^{\lambda\mu} = \frac{1}{2}\sum_{\lambda\mu i}\sum_{q}(\phi^{\lambda\mu i}_{qq'})^2.$$

The values of greatest interest are the maximum values of n_q and $n_q^{\lambda\mu}$ with respect to q. We have calculated these values for ^{168}Er, ^{156}Gd and ^{228}Th with the following results:

^{168}Er	$\pi411\downarrow$:	$(n_q^{22})_{max} = 0.016$
		$(n_q)_{max} = 0.017$
	$\nu521\downarrow$:	$(n_q^{20})_{max} = 0.001$
	$\pi400\uparrow$:	$(n_q^{30})_{max} = 0.0025$
	$\nu633\uparrow$:	$(n_q^{31})_{max} = 0.0027$
^{156}Gd	$\nu660\uparrow$:	$(n_q^{20})_{max} = 0.03$
		$(n_q)_{max} = 0.04$
	$\pi411\downarrow$:	$(n_q^{22})_{max} = 0.014$
	$\pi411\uparrow$:	$(n_q^{30})_{max} = 0.014$
	$\pi532\uparrow$:	$(n_q^{31})_{max} = 0.024$
^{228}Th	$\pi651\uparrow$:	$(n_q^{20})_{max} = 0.047$
		$(n_q^{30})_{max} = 0.034$
		$(n_q)_{max} = 0.085$
	$\pi530\uparrow$:	$(n_q^{20})_{max} = 0.032$
		$(n_q^{30})_{max} = 0.015$
		$n_q = 0.048$
	$\nu633\downarrow$:	$(n_q^{30})_{max} = 0.041$
		$n_q = 0.045$

The ground-state correlations increase from ^{168}Er to ^{156}Gd, with the largest contributions coming from the gamma-vibrational state and from the 0^+ states, respectively. Nevertheless, in both these nuclei the ground state

correlations are small and the RPA can be expected to give a good description of low-lying vibrational states. In ^{228}Th the number of quasiparticles in the ground state increases compared to ^{168}Er by a factor of ~ 5, giving a relatively strong contribution to the ground state wave function.

In [23] the three-phonon terms have been added to the wave function and their role has been investigated. In the approximation used there the three-phonon terms lead to a shift of the two-phonon poles which we denote by $\Delta(\lambda_1\mu_1 i_1, \lambda_2\mu_2 i_2)$. This shift has been calculated in [30]. For ^{168}Er one obtains

$$\Delta(\lambda_1\mu_1 i_1, \lambda_2\mu_2 i_2) = -0.2\Delta\omega(\lambda_1\mu_1 i_1, \lambda_2\mu_2 i_2),$$

whereas our calculation for ^{228}Th yields

$$\Delta(\lambda_1\mu_1 i_1, \lambda_2\mu_2 i_2) = -(0.2 \div 0.4)\Delta\omega(\lambda_1\mu_1 i_1, \lambda_2\mu_2 i_2).$$

This result, as well as the increased ground state correlations, means that the accuracy of the calculation in ^{228}Th is worse than in the well deformed nuclei ^{168}Er and ^{238}U.

3.2.3 Numerical results

The calculated energies of the nonrotational states (bandheads) are compared in Table 8 with the experimental results. The structure of the calculated levels is given as contributions of the one-phonon $(\lambda\mu)_i$ and two-phonon $\{(\lambda_1\mu_1)_{i_1}, (\lambda_2\mu_2)_{i_2}\}$ components to the normalization of the wave function (eqs. (9) and (10)). The Pauli principle is taken into account in the contribution of two-phonon components. The results of the calculation for those states, for which no reliable experimental assignments can be made up to now, are listed in Table 9. All the calculated nonrotational states with energies below 1.8 MeV and some selected states above 1.8 MeV are given in the two tables.

The energy of the first $K^\pi = 0^-$ state calculated with $\kappa_0^{30} = 0.0128$ fm^{2}MeV^{-1} is 0.17 MeV larger than the experimental energy. A calculation with $\kappa_0^{30} = 0.0131$ fm^{2}MeV^{-1}, as was used in ^{238}U, gives an energy of 0.4 MeV for the $K^\pi = 0^-$ state and $B(E3)\uparrow = 100$ W.u. and $B(E1)\uparrow = 1.4 \cdot 10^{-2}$ W.u.. In this case, however, the ground state correlation and a shift of a two-phonon pole increased. Therefore we used the smaller value of κ_0^{30} in the present calculation.

The contributions of the largest two-quasineutron ($\nu\nu$) and two-quasiproton ($\pi\pi$) components to the wave functions of the one-phonon states $(\lambda\mu)_i$ are listed in Table 10. Only the components ≥ 2 % are included, which account in most cases for more than $\sim$80 % of the wave function. A few levels, however, are very collective -notably the first three $K^\pi = 0^-$ states- and therefore their wave functions have many small components not listed in the table.

The $E1$, $E2$ and $M1$ transition rates between excited states in ^{228}Th, calculated in the QPNM, are given in Table 11.

Table 8. Comparison of the observed levels in ^{228}Th with the predictions of the quasiparticle-phonon nuclear model

Experiment		Calculation in the QPNM		
K_n^π	E_n MeV	E_n MeV	$B(\sigma\lambda)\uparrow$ [b] W.u.	Structure (%)[a]
0_1^-	0.328	0.5	$B(E3) = 60$ $B(E1) = 7.5 \cdot 10^{-3}$	$(30)_1$ 99
0_1^+	0.832	0.8	$B(E2) = 1$	$(20)_1$ 97 $\{(30)_1, (30)_2\}$ 0.3
0_2^+	0.939	1.0	$B(E2) = 0.2$	$(20)_2$ 95; $(20)_1$ 0.8 $\{(30)_1, (30)_1\}$ 0.7
1_1^-	0.944	1.0	$B(E3) = 30$ $B(E1) = 5.0 \cdot 10^{-5}$	$(31)_1$ 98 $\{(20)_2, (30)_1\}$ 1
2_1^+	0.969	1.0	$B(E2) = 11$	$(22)_1$ 98
0_3^+	1.120	1.2	$B(E2) = 0.8$	$(20)_3$ 82; $(20)_4$ 14 $(20)_2$ 1
2_1^-	1.123	1.2	$B(E3) = 9$	$(32)_1$ 97 $\{(22)_1, (30)_1\}$ 2
2_2^+	1.153	1.3	$B(E2) = 0.6$	$(22)_2$ 99
1_1^+	1.393	1.4	$B(E2) = 0.01$ $B(M1) = 1.7 \cdot 10^{-4}$	$(21)_1$ 98 $\{(30)_1, (31)_1\}$ 1
3_1^-	1.344	1.4	$B(E3) = 21$	$(33)_1$ 95 $\{(20)_1, (33)_1\}$ 3
2_3^+	(1.416)	1.5	$B(E2) = 2.5$	$(22)_3$ 96 $\{(30)_1, (32)_1\}$ 2
4_1^+	1.432	1.5	$B(E4) = 15$	$(44)_1$ 99
4_1^-	1.450	1.5	$B(E5) = 20$	$(54)_1$ 99
3_1^+	1.531	1.6	$B(E4) = 40$	$(43)_1$ 91 $\{(30)_1, (33)_1\}$ 7
4_2^+	(1.744)	1.8	$B(E4) = 6$	$(44)_2$ 98
3_2^+	(1.945)	1.9	$B(E4) = 0.03$	$(43)_2$ 87; $(43)_3$ 9

a) Phonons denoted by $(\lambda\mu)_i$ where i is the root number (see text)
b) $B(\sigma\lambda)\uparrow = (2 - \delta_{K,0})\langle K|\mathcal{M}(\sigma\lambda, K)|0_g\rangle^2$, in Weisskopf-units [16]

3.2.4 Discussion of the QPNM results

The energies of the nonrotational octupole states in ^{228}Th are well described in the QPNM (except for the first $K^\pi = 0^-$ state). The computed first- and second-excited states for $K^\pi = 0^-$, 1^-, 2^- and 3^- have a collective vibrational character.

For the $0^+0_g \rightarrow 1^-K_1$ $E1$ transitions the calculation yields matrix elements of

$$\langle 0_g^+|\mathcal{M}(E1,0)|0_1^-\rangle = 0.13\,\mathrm{e}\cdot\mathrm{fm} \text{ and}$$
$$\langle 0_g^+|\mathcal{M}(E1,-1)|1_1^-\rangle = 0.008\,\mathrm{e}\cdot\mathrm{fm}.$$

The matrix element for the $K^\pi = 0^-$ state is a factor of 2 larger than the observed one, whereas there is agreement between the experimental and calculated results for the

Table 10. Two-quasiparticle configurations of the one-phonon-states

$(\lambda\mu)_i^a$	two-quasiparticle components (%)^b				
$(20)_1$	$\pi\pi 530\uparrow-530\uparrow$ 58	$\nu\nu 633\downarrow-633\downarrow$ 31	$\pi\pi 402\downarrow-402\downarrow$ 3	$\pi\pi 660\uparrow-660\uparrow$ 2	$\pi\pi 651\uparrow-651\uparrow$ 2
$(20)_2$	$\nu\nu 633\downarrow-633\downarrow$ 45	$\nu\nu 631\uparrow-631\uparrow$ 20	$\pi\pi 530\uparrow-530\uparrow$ 8	$\pi\pi 532\downarrow-532\downarrow$ 2	
$(20)_3$	$\nu\nu 631\uparrow-631\uparrow$ 67	$\pi\pi 651\uparrow-651\uparrow$ 4	$\nu\nu 633\downarrow-633\downarrow$ 2	$\pi\pi 402\downarrow-402\downarrow$ 2	$\pi\pi 660\uparrow-660\uparrow$ 2
$(20)_4$	$\pi\pi 651\uparrow-651\uparrow$ 30	$\pi\pi 660\uparrow-660\uparrow$ 19	$\pi\pi 402\downarrow-402\downarrow$ 19	$\nu\nu 633\downarrow-633\downarrow$ 10	$\pi\pi 660\uparrow-640\uparrow$ 6 $\nu\nu 770\uparrow-770\uparrow$ 3
$(20)_5$	$\pi\pi 660\uparrow-660\uparrow$ 23	$\nu\nu 752\uparrow-752\uparrow$ 15	$\pi\pi 402\downarrow-402\downarrow$ 12	$\pi\pi 651\uparrow-651\uparrow$ 11	$\nu\nu 631\uparrow-631\uparrow$ 8
$(20)_6$	$\pi\pi 660\uparrow-660\uparrow$ 38	$\pi\pi 402\downarrow-402\downarrow$ 12	$\pi\pi 651\uparrow-651\uparrow$ 11	$\nu\nu 752\uparrow-752\uparrow$ 4	$\nu\nu 631\uparrow-631\uparrow$ 2
$(20)_7$	$\pi\pi 770\uparrow-770\uparrow$ 23	$\nu\nu 503\downarrow-503\downarrow$ 10	$\pi\pi 660\uparrow-660\uparrow$ 9	$\pi\pi 402\downarrow-402\downarrow$ 6	
$(20)_8$	$\pi\pi 532\downarrow-532\downarrow$ 60	$\pi\pi 651\uparrow-651\uparrow$ 12	$\pi\pi 642\uparrow-642\uparrow$ 6	$\pi\pi 660\uparrow-400\uparrow$ 3	$\pi\pi 400\uparrow-400\uparrow$ 2
$(21)_1$	$\pi\pi 532\downarrow-530\uparrow$ 99				
$(21)_2$	$\nu\nu 633\downarrow-631\uparrow$ 98				
$(22)_1$	$\nu\nu 633\downarrow-630\uparrow$ 66	$\nu\nu 743\uparrow-761\uparrow$ 13	$\pi\pi 532\downarrow+530\uparrow$ 5	$\pi\pi 642\uparrow-400\uparrow$ 3	
$(22)_2$	$\nu\nu 743\uparrow-761\uparrow$ 60	$\nu\nu 633\downarrow-631\downarrow$ 28	$\pi\pi 532\downarrow+530\uparrow$ 5	$\pi\pi 642\uparrow-400\uparrow$ 2	
$(22)_3$	$\pi\pi 532\downarrow+531\downarrow$ 62	$\nu\nu 743\uparrow-761\uparrow$ 22	$\pi\pi 642\uparrow-400\uparrow$ 6	$\nu\nu 633\downarrow-631\downarrow$ 3	
$(22)_4$	$\pi\pi 642\uparrow-400\uparrow$ 72	$\pi\pi 532\downarrow+530\uparrow$ 20	$\nu\nu 743\uparrow-761\uparrow$ 2		
$(22)_5$	$\pi\pi 651\uparrow+660\uparrow$ 84	$\nu\nu 642\uparrow-400\uparrow$ 6	$\pi\pi 532\downarrow+530\uparrow$ 2	$\nu\nu 631\uparrow+631\downarrow$ 2	
$(30)_1$	$\nu\nu 752\uparrow-633\downarrow$ 69	$\pi\pi 530\uparrow-660\uparrow$ 4	$\pi\pi 521\uparrow-651\uparrow$ 5		
$(30)_2$	$\nu\nu 752\uparrow-633\downarrow$ 27	$\pi\pi 532\downarrow-651\uparrow$ 20	$\pi\pi 530\uparrow-660\uparrow$ 15	$\pi\pi 530\uparrow-400\uparrow$ 9	$\pi\pi 521\uparrow-651\uparrow$ 6 $\nu\nu 761\uparrow-631\uparrow$ 4
$(30)_3$	$\pi\pi 532\downarrow-651\uparrow$ 76	$\pi\pi 530\uparrow-400\uparrow$ 10	$\pi\pi 530\uparrow-660\uparrow$ 6		
$(31)_1$	$\pi\pi 651\uparrow-530\uparrow$ 80	$\nu\nu 743\uparrow-633\downarrow$ 4	$\nu\nu 752\uparrow-631\uparrow$ 4		
$(31)_2$	$\nu\nu 752\uparrow-631\uparrow$ 64	$\pi\pi 651\uparrow-530\uparrow$ 14	$\nu\nu 743\uparrow-633\downarrow$ 12		
$(31)_3$	$\nu\nu 743\uparrow-633\downarrow$ 64	$\nu\nu 752\uparrow-631\uparrow$ 26	$\pi\pi 651\uparrow-530\uparrow$ 2		
$(32)_1$	$\pi\pi 651\uparrow+530\uparrow$ 91	$\pi\pi 642\uparrow-530\uparrow$ 2	$\nu\nu 743\uparrow-631\uparrow$ 2		
$(32)_2$	$\nu\nu 743\uparrow-631\uparrow$ 72	$\pi\pi 642\uparrow-530\uparrow$ 11	$\pi\pi 651\uparrow+530\uparrow$ 6	$\pi\pi 523\downarrow-400\uparrow$ 2	
$(33)_1$	$\pi\pi 642\uparrow+530\uparrow$ 76	$\nu\nu 633\downarrow+501\downarrow$ 5	$\pi\pi 651\uparrow+532\downarrow$ 2		
$(33)_2$	$\pi\pi 532\downarrow+651\uparrow$ 48	$\nu\nu 633\downarrow+501\downarrow$ 25	$\pi\pi 642\uparrow+530\uparrow$ 16		
$(43)_1$	$\nu\nu 642\downarrow+631\uparrow$ 22	$\pi\pi 523\downarrow+530\uparrow$ 18	$\pi\pi 642\uparrow+400\uparrow$ 4	$\nu\nu 743\uparrow-501\downarrow$ 4	$\pi\pi 651\uparrow+402\downarrow$ 3
$(43)_2$	$\nu\nu 642\downarrow+631\uparrow$ 48	$\pi\pi 651\uparrow+402\downarrow$ 45	$\pi\pi 523\downarrow+530\uparrow$ 3		
$(43)_3$	$\pi\pi 651\uparrow+402\downarrow$ 50	$\nu\nu 642\downarrow+631\uparrow$ 27	$\pi\pi 523\downarrow+530\uparrow$ 14		
$(44)_1$	$\nu\nu 633\downarrow+631\uparrow$ 65	$\nu\nu 622\uparrow+631\uparrow$ 16	$\nu\nu 752\uparrow+761\uparrow$ 6	$\pi\pi 651\uparrow+642\uparrow$ 4	
$(44)_2$	$\nu\nu 752\uparrow+761\uparrow$ 32	$\nu\nu 633\downarrow+631\uparrow$ 31	$\nu\nu 633\downarrow+642\downarrow$ 7	$\pi\pi 642\uparrow+651\uparrow$ 4	$\nu\nu 622\uparrow+631\uparrow$ 3
$(54)_1$	$\nu\nu 761\uparrow+633\downarrow$ 48	$\pi\pi 532\downarrow+642\uparrow$ 17	$\pi\pi 523\downarrow+651\uparrow$ 11	$\nu\nu 752\uparrow+642\downarrow$ 3	
$(54)_2$	$\nu\nu 761\uparrow+633\downarrow$ 41	$\pi\pi 532\downarrow+642\uparrow$ 36	$\nu\nu 752\uparrow+631\uparrow$ 15	$\pi\pi 523\downarrow+651\uparrow$ 5	
$(55)_1$	$\nu\nu 752\uparrow+633\downarrow$ 100				

a) Phonons denoted by $(\lambda\mu)_i$ where i is the root number (see text)
b) Nilsson orbitals denoted by their asymptotic quantum numbers

$K^\pi = 1^-$ state. It is interesting to note that the $B(E1)$ for the $\Delta K = 0$ transition is close in magnitude to those observed and calculated for the corresponding transitions in the rare-earth region [31,32].

For the $M1$ and $E2$ transitions between the $K^\pi = 1^-$ and 0^- bands we obtain matrix elements of

$$\langle 0_1^- | \mathcal{M}(M1,-1) | 1_1^- \rangle = 0.59\,\mu_N$$
$$\langle 0_1^- | \mathcal{M}(E2,-1) | 1_1^- \rangle = 0.2\,\mathrm{e}\cdot\mathrm{fm}^2$$

These values are consistent with the experimental results as discussed in Sec. 3.1.

For the transitions from the $K_n^\pi = 2_1^-$ band to the $K_n^\pi = 2_1^+$ and 0_1^- bands we obtain a ratio of $E1$ to $E2$ matrix elements of $3.1 \cdot 10^{-3}$ fm^{-1} in excellent agreement with the experimental result (see Table 5). According to our calculation the wave function of the $K_n^\pi = 2_1^-$ state has 97 % of the one-phonon $(32)_1$ and 2 % of the two-phonon

Table 9. Levels predicted in the quasiparticle-phonon nuclear model wich are not observed experimentally

K^π_n	E_n MeV	$B(\sigma\lambda)\uparrow$ [b] W.u.	Structure (%)[a]
0^+_4	1.4	$B(E2) = 2$	$(20)_4$ 78 ; $(20)_3$ 17
1^-_2	1.5	$B(E3) = 13$ $B(E1) = 1.2 \cdot 10^{-3}$	$(31)_2$ 98
0^+_5	1.6	$B(E2) = 0.3$	$(20)_5$ 97 ; $(20)_4$ 1 $\{(30)_1, (30)_1\}$ 0.5
1^+_2	1.6	$B(E2) = 0.1$ $B(M1) = 1.1 \cdot 10^{-2}$	$(21)_2$ 99
0^-_2	1.6	$B(E3) = 14$ $B(E1) = 2.1 \cdot 10^{-3}$	$(30)_2$ 96 $\{(20)_1, (30)_1\}$ 2
5^-_1	1.7		$(55)_1$ 100
2^-_2	1.7	$B(E3) = 9$	$(32)_2$ 97 $\{(22)_1, (30)_1\}$ 1
3^-_2	1.7	$B(E3) = 3$	$(33)_2$ 81 ; $(33)_3$ 11
0^+_6	1.7	$B(E2) = 0.6$	$(20)_6$ 92 $\{(30)_1, (30)_1\}$ 4
2^+_4	1.7	$B(E2) = 1.5$	$(22)_4$ 98
1^-_3	1.7	$B(E3) = 0.7$ $B(E1) = 2.5 \cdot 10^{-4}$	$(31)_3$ 97 $\{(20)_1, (31)_1\}$ 2
0^-_3	1.8	$B(E3) = 2$ $B(E1) = 1.7 \cdot 10^{-4}$	$(30)_3$ 68 $\{(20)_3, (30)_1\}$ 16 $\{(20)_2, (30)_1\}$ 10
0^+_7	1.8	$B(E2) = 3$	$(20)_7$ 97 $\{(30)_1, (30)_1\}$ 0.2
2^+_5	1.9	$B(E2) = 0.2$	$(22)_5$ 70 $\{(30)_1\ (32)_1\}$ 27
0^+_8	1.9	$B(E2) = 0.04$	$(20)_8$ 74 ; $(20)_9$ 4 $(20)_6$ 4
4^-_2	1.9	$B(E5) = 2$	$(54)_2$ 99
3^+_3	2.0	$B(E4) = 1.4$	$(43)_3$ 79 ; $(43)_2$ 8 $\{(30)_1, (33)_1\}$ 7

a) Phonons denoted by $(\lambda\mu)_i$ where i is the root number (see text)
b) $B(\sigma\lambda)\uparrow = (2 - \delta_{K,0})\langle K|\mathcal{M}(\sigma\lambda, K)|0_g\rangle^2$, in Weisskopf-units [16]

Table 11. $E1$, $E2$ and $M1$ transition rates between excited states in ^{228}Th, calculated in the QPNM.

Initial state		Final state		$E\lambda$ or $M1$ (MeV)	$B(E\lambda)$, e^{2}fm$^{2\lambda}$ or $B(M1)$, μ_N^2
$I^\pi K_n$	E_n (MeV)	$I^\pi K_n$	E_n		
0^+0_1	0.87	1^-0_1	0.5	$E1$	$1.6{\cdot}10^{-4}$
0^+0_2	1.0	1^-0_1	0.5	$E1$	$9.2{\cdot}10^{-4}$
1^-1_1	1.0	1^-0_1	0.5	$M1$	0.35
3^-1_1	1.1	1^-0_1	0.5	$E2$	$2.1{\cdot}10^{-2}$
0^+0_3	1.2	1^-0_1	0.5	$E1$	$9.2{\cdot}10^{-5}$
2^-2_1	1.2	1^-0_1	0.5	$E2$	5.0
2^-2_1	1.2	2^+2_1	1.0	$E1$	$9.4{\cdot}10^{-5}$
2^+2_2	1.3	0^+0_1	0.87	$E2$	0.54
2^+2_2	1.3	0^+0_2	1.2	$E2$	0.12
2^+2_2	1.3	2^+2_1	1.0	$E2$	0.51
2^+2_2	1.3	2^+2_1	1.0	$M1$	$3.2{\cdot}10^{-2}$
4^+4_1	1.43	2^+2_1	1.0	$E2$	0.31
4^+4_1	1.43	2^+2_2	1.3	$E2$	$1.0{\cdot}10^{-2}$
4^-4_1	1.45	3^-3_1	1.5	$M1$	$8.2{\cdot}10^{-4}$
4^-4_1	1.45	3^-3_1	1.35	$E2$	$5.8{\cdot}10^{-5}$
4^-4_1	1.45	4^+4_1	1.43	$E1$	$9.4{\cdot}10^{-5}$
4^-4_1	1.45	2^-2_1	1.12	$E2$	0.22
1^-1_2	1.5	1^-0_1	0.5	$M1$	0.42
3^+3_1	1.6	2^+2_1	1.0	$M1$	$5.7{\cdot}10^{-2}$
3^+3_1	1.6	4^+4_1	1.5	$M1$	$5.1{\cdot}10^{-3}$
3^+3_1	1.6	2^+2_1	1.0	$E2$	0.31
3^+3_1	1.6	1^-0_1	0.5	$E3$	$3.1{\cdot}10^{3}$
4^+3_1	1.7	1^-0_1	0.5	$E3$	804
3^-2_2	1.8	1^-0_1	0.5	$E2$	0.81
4^+4_2	1.8	2^+2_1	1.0	$E2$	3.1
2^+2_5	1.9	2^-2_1	1.2	$E1$	$3.9{\cdot}10^{-3}$
4^+3_2	1.95	1^-0_1	0.5	$E3$	39
4^+3_3	2.0	1^-0_1	0.5	$E3$	360

$\{(22)_1, (30)_1\}$ components, and the calculated $E1/E2$ ratio depends strongly on this composition.

The computed energies of the three excited $K^\pi = 0^+$ and two $K^\pi = 2^+$ bands are in agreement with the observed ones. The wave functions of the 0^+ states are a superposition of a large number of two-quasiparticle configurations. We note that the magnitude of the $B(E2)$ values for the transitions from the ground state to these states is not correlated with the degree of their two-quasiparticle composition, as was already observed earlier [22,26].

The calculated ratios of the $E1$ to $E2$ transition matrix elements from the 0^+_1, 0^+_2 and 0^+_3 states to the octupole 0^-_1 and ground states are compared with the experimental ones in Table 5. The small admixtures of the two-phonon components to the wave functions of the 0^+_1 and 0^+_2 states (0.3 % $\{(30)_1, (30)_2\}$, 0.7 % $\{(30)_1, (30)_1\}$ and $\leq$ 0.1 % to the wave functions of the 0^+_1, 0^+_2 and 0^+_3 states, respectively), are responsible for the fast $E1$ transitions. Our calculation thus demonstrates that small components of the wave functions can strongly enhance the $E1$ transition rates. Since as a rule only the largest components of the wave functions of excited states are described correctly in the QPNM and other microscopic calculations, the reasonable agreement of the experimental and calculated $B(E1)/B(E2)$ ratios is quite satisfactory.

The first $K^\pi = 2^+$ state is a collective gamma-vibrational state as in all deformed nuclei. The wave functions of the next four 2^+ states in ^{228}Th are superpositions of many two-quasiparticle components. However, again the $E2$ transitions to these states are not necessarily enhanced, and the $B(E2)\uparrow$ for the second-excited $K^\pi = 2^+$ state is small in agreement with experiment. This latter state decays predominantly by $E0$ transitions to the gamma-vibrational state as discussed in [2]. Our calcula-

tion yields for the monopole strength parameter

$$\rho^2(E0; 2^+2_2 \rightarrow 2^+2_1) = 8 \cdot 10^{-4}$$

which is 3 times smaller than the experimental result.

According to our calculation the first two $K^\pi = 1^+$ states have essentially pure two-quasiparticle character. The computed $M1$ strength summed over the energy region from 2.1 to 2.5 MeV equals 3.2 μ_N^2. This value is almost identical to that calculated earlier for ^{238}U [27] which was found to be in agreement with experiment. Thus the total $M1$ strength in the low-energy region in ^{228}Th can be expected to be close to that in ^{238}U.

The first two $K^\pi = 4^+$ states are predicted to be one-phonon $(44)_i$ (hexadecapole) states with less than 1 % two-phonon $\{(22)_1, (22)_2)\}$ contents, and the first $K^\pi = 4^-$ state is a one-phonon $(54)_1$ state. Their wave functions are superpositions of several two-quasiparticle components. The $E2$ transitions between the $K_n^\pi = 4_1^+$, 4_2^+ and $K^\pi = 2_1^+$, 2_2^+ states are weak. The computed ratio $B(E2; 4^+4_1 \rightarrow 2^+2_1)/B(E2; 4^+4_1 \rightarrow 2^+2_2) = 30$ is approx. three times larger than the experimental one. The computed ratio of the $(4_1^- \rightarrow 4_1^+)$ $E1$ to $(4_1^- \rightarrow 2_1^-)$ $E2$ transition matrix element is 2.5 times larger than the experimental value (see Table 5).

Finally, the first $K^\pi = 3^+$ state is predicted to have predominantly a one-phonon $(43)_1$ (hexadecapole) structure with a 7 % admixture of the two-phonon $\{(30)_1, (33)_1\}$ excitation. Its decay by $M1$ transitions to the 4_1^+ and 2_1^+ states constitutes the only serious discrepancy between experiment and theory: the ratio $\frac{B(M1,3^+\rightarrow 4^+)}{B(M1,3^+\rightarrow 2^+)}$ has experimental and computed values of approx. 1000 and 1/10, respectively. We note, however, that the calculated $B(M1)'$s result from transitions between very small two-quasiparticle components of the wave functions, which are sensitive to $\kappa_0^{\lambda\mu}$ and β_2.

The nuclear levels in ^{228}Th are populated in the β^- decay of ^{228}Ac and the electron capture decay of ^{228}Pa. Both these odd-odd nuclei have a $I^\pi K = 3^+3$ ground state, and for both ground states the configuration $(\pi 651\uparrow + \nu 631\uparrow)$ has been suggested [21,33]. We have calculated the β-decay matrix elements of the allowed Gamow-Teller transitions to levels with $I^\pi K = 2^+2$, 3^+3 and 4^+4 which are termed allowed hindert. The calculated β-decay rates are faster, as a rule, than the experimental ones. We will therefore restrict our discussion to a comparison of the ratios of β matrix elements.

In heavy nuclei transitions between spin-orbit partners are the only allowed β-transitions with nonvanishing matrix elements for the asymptotic wave functions. In the present case this would be transitions to 2^+ levels with the configurations $\pi\pi 651\uparrow + 631\downarrow$ for the ^{228}Ac decay and $\nu\nu 651\downarrow + 631\uparrow$ for the ^{228}Pa decay. The first two $K^\pi = 2^+$ states in ^{228}Th do not contain such configurations, but must be pupulated through very small components. Therefore the $\log ft$ values are predicted to be very large in agreement with the experimental data.

Table 12. Ratios of the matrix elements for β-transitions from $K^\pi = 3^+(\pi 651\uparrow + \nu 631\uparrow)$ of ^{228}Pa and ^{228}Ac to $K_n^\pi = 3_1^+$, 3_2^+ and $K_n^\pi = 4_1^+$, 4_2^+ states of ^{228}Th

	experiment[a]	calculation
$\frac{\lvert\mathcal{M}(3^{+\,228}\mathrm{Pa} \xrightarrow{\beta^+} 3_1^{+\,228}\mathrm{Th})\rvert}{\lvert\mathcal{M}(3^{+\,228}\mathrm{Ac} \xrightarrow{\beta^-} 3_1^{+\,228}\mathrm{Th})\rvert}$	0.23(2)	0.2
$\frac{\lvert\mathcal{M}(3^{+\,228}\mathrm{Pa} \xrightarrow{\beta^+} 3_2^{+\,228}\mathrm{Th})\rvert}{\lvert\mathcal{M}(3^{+\,228}\mathrm{Ac} \xrightarrow{\beta^-} 3_2^{+\,228}\mathrm{Th})\rvert}$	0.63(4) 3.0(3) 2.7(1)	0.7
$\frac{\lvert\mathcal{M}(3^{+\,228}\mathrm{Pa} \xrightarrow{\beta^+} 3_1^{+\,228}\mathrm{Th})\rvert}{\lvert\mathcal{M}(3^{+\,228}\mathrm{Pa} \xrightarrow{\beta^+} 3_2^{+\,228}\mathrm{Th})\rvert}$	0.11(1) 0.15(2) 0.075(7)	0.3
$\frac{\lvert\mathcal{M}(3^{+\,228}\mathrm{Ac} \xrightarrow{\beta^-} 3_1^{+\,228}\mathrm{Th})\rvert}{\lvert\mathcal{M}(3^{+\,228}\mathrm{Ac} \xrightarrow{\beta^-} 3_2^{+\,228}\mathrm{Th})\rvert}$	0.75(5) 1.9(2) 0.85(3)	1.0
$\frac{\lvert\mathcal{M}(3^{+\,228}\mathrm{Pa} \xrightarrow{\beta^+} 4_1^{+\,228}\mathrm{Th})\rvert}{\lvert\mathcal{M}(3^{+\,228}\mathrm{Ac} \xrightarrow{\beta^-} 4_1^{+\,228}\mathrm{Th})\rvert}$	5.0(13)	1.3
$\frac{\lvert\mathcal{M}(3^{+\,228}\mathrm{Pa} \xrightarrow{\beta^+} 4_2^{+\,228}\mathrm{Th})\rvert}{\lvert\mathcal{M}(3^{+\,228}\mathrm{Ac} \xrightarrow{\beta^-} 4_2^{+\,228}\mathrm{Th})\rvert}$	0.80(3)	0.96
$\frac{\lvert\mathcal{M}(3^{+\,228}\mathrm{Pa} \xrightarrow{\beta^+} 4_1^{+\,228}\mathrm{Th})\rvert}{\lvert\mathcal{M}(3^{+\,228}\mathrm{Pa} \xrightarrow{\beta^+} 4_2^{+\,228}\mathrm{Th})\rvert}$	3.3(2)	3.5
$\frac{\lvert\mathcal{M}(3^{+\,228}\mathrm{Ac} \xrightarrow{\beta^-} 4_1^{+\,228}\mathrm{Th})\rvert}{\lvert\mathcal{M}(3^{+\,228}\mathrm{Ac} \xrightarrow{\beta^-} 4_2^{+\,228}\mathrm{Th})\rvert}$	0.54(14)	2.5

a)From present work and [6]. The experimental results are for the 3^+ levels at 1646, 1893 and 1945 keV (first, second and third listed number, respectively) and the 4^+ level at 1744 keV

The calculated ratios of the β decay matrix elements to the first two $K^\pi = 3^+$ and 4^+ states are compared with experimental values in Table 12. For the second-excited 3^+ state we have listed the experimental results for the three levels at 1646, 1893 and 1945 keV (see table 7). The calculation gives 3^+ states at 1.61, 1.94, 1.98 and 2.12 MeV. These levels could be slightly lowered ($\approx 0.1\ MeV$) by small changes of β_2 since the energies of several single-particle levels close to the Fermi level depend strongly on the deformation. However, major changes of the single particle levels would be nescessary to obtain the 3_2^+ state at 1646 keV.

The calculated ratio of the β^+ and β^- matrix elements for the transitions to the $K_n^\pi = 3_1^+$ state is in agreement with the experimental ratio. This ratio is not sensitive to the equilibrium deformation and the constant κ_0^{43}. Thus the observed large difference of the ft values between the β decays of ^{228}Ac and ^{228}Pa with the same two-quasiparticle configuration can be described satisfactorily. The other ratios of matrix elements listed in Table 12 are rather sensitive to β_2 and the constants κ_0^{43} and κ_0^{44}, but the exper-

imental trends are also described at least qualitatively by the calculation.

4 Conclusion

The level structure of ^{228}Th was studied in the EC decay of ^{228}Pa, and compared to the predictions of the quasiparticle-phonon nuclear model. There is a surprisingly close agreement between experiment and theory: from the 16 nonrotational states predicted below 1.6 MeV all except two - a forth $K^\pi = 0^+$ state at 1.4 MeV and a second $K^\pi = 1^-$ state at 1.5 MeV - are experimentally observed. Particularly noteworthy is the satisfactory prediction of both the bandhead energies and the electromagnetic decay properties of the three lowest excited $K^\pi = 0^+$ bands and the two excited 2^+ bands. The 0^+ states are particularly difficult to calculate, and the structure of the second-excited 2^+ band, which is also observed in the neighbouring nuclei, has to our knowledge not been explained satisfactorily so far (see e.g. [34]).

The QPNM calculations for ^{228}Th are nontrivial. The density of the single-particle levels around the Fermi-surface is high in this nucleus, and there are quasicrossings between them. The results of the calculations are sensitive to the deformation parameters and the isoscalar constants of the multipole interactions. Therefore the description of the nonrotational states of ^{228}Th within the QPNM is worse, and the predictions are less reliable than in well-deformed nuclei. Moreover, ^{228}Th was often considered to be a transitional nucleus, and the QPNM cannot be used for the description of levels in such nuclei without modifications. We therefore conclude from the satisfactory agreement of the calculated and observed level structure that ^{228}Th is not a typical transitional nucleus, but a specific deformed nucleus with very low-lying first $K^\pi = 0^-$ and 0^+ excitations.

We believe that the low-energy part of the level structure of ^{228}Th is now established. Many questions remain, however, above $\sim$ 1.6 MeV where we could not identify reliably any rotational bands. Our data indicate that additional as yet unidentified levels might be weakly populated both in the ^{228}Ac and ^{228}Pa decays between 1.6 and 2 MeV. It would be worthwile to reinvestigate these decays with one of the large γ-ray detector arrays.

Another unsolved problem is the theoretical description of the moments of inertia of the observed rotational bands. These observables show some very distinct features, but unfortunately we have no code for a resonably good calculation of the moments of inertia of vibrational states within the QPNM.

This work was partly funded by the DFG grants Bo 1109/1 (J.d.B.), Gu 179/3-4 (T.W., J.G., C.G.), He 1316/3-1 (J.G., P.H.), by the grant RFFR 96-15-96729 (V.G.S., A.V.S., N.Yu.S.) and by the Forschungszentrum Karlsruhe GmbH - Technik und Umwelt.

References

1. Kurcewicz, W., Stryczniewicz, K., Żylicz, J., Broda, R., Chojnacki, S., Walus, W., Yutlandov, I.: J. Phys. (Paris) 34, 159 (1973)
2. Baltzer, H., Freitag, K., Günther, C., Herzog, P., Manns, J., Müller, U., Paulsen, R., Sevenich, P., Weber, T., Will, B.: Z. Phys. A 352, 47 (1995)
3. Dalmasso, J., Maria, H., Ardisson, G.: Phys. Rev. C36, 2510 (1987)
4. Weber, T., deBoer, J., Freitag, K., Gröger, J., Günther, C., Manns, J., Müller, U.: Z. Phys. A 358, 281 (1997)
5. Weber, T.: Ph.D. thesis, University of Bonn (1998)
6. Artna-Cohen, A: Nuclear Data Sheets 80, 723 (1997)
7. Steffen, R.M., Alder, K. in: The electromagnetic interaction in nuclear spectroscopy. Hamilton, W.D. ed., Amsterdam: North-Holland (1975)
8. Krane, K.S., Steffen, R.M.: Phys. Rev. C2, 724 (1970)
9. Baltzer, H., deBoer, J., Gollwitzer, A., Graw, G., Günther, C., Levon, A.I., Loewe, M., Maier, H.J., Manns, J., Müller, U., Valnion, B.D., Weber, T., Würkner, M.: Z. Phys. A356, 13 (1996)
10. Ackermann, B., Baltzer, H., Freitag, K., Günther, C., Herzog, P., Manns, J., Müller, U., Paulsen, R., Sevenich, P., Weber, T., Will, B., deBoer, J., Graw, G., Levon, A.I., Loewe, M., Lösch, A., Müller-Zanotti, E.: Z. Phys. A 350, 13 (1994)
11. McGowan, F.K., Milner, W.T.: Nucl. Phys. A 562, 241 (1993)
12. Kröll, Th.: Ph.D. thesis, University of Frankfurt (1996)
13. Schmorak, M.R.: Nuclear Data Sheets 63, 139 (1991)
14. Ackermann, B., Baltzer, H., Ensel, C., Freitag, K., Grafen, V., Günther, C., Herzog, P., Manns, J., Marten-Tölle, M., Müller, U., Prinz, J., Romanski, I., Tölle, R., deBoer, J., Gollwitzer, N., Maier, H.J.: Nucl. Phys. A559, 61 (1993)
15. Rösel, F., Fries, H.M., Alder, K., Pauli, H.C.: Atomic Data and Nuclear Data Tables 21, 291 (1978)
16. Bohr, A., Mottelson, B.R.: Nuclear structure. Vol. I: New York: Benjamin (1969); Vol. II. Reading, Mass.: Benjamin (1975)
17. Weber, T., Gröger, J., Günther, C., deBoer, J.: Eur. Phys. J. A 1, 39 (1997)
18. McGowan, F.K., Bemis, Jr., C.E., Milner, W.T., Ford, Jr., J.L.C., Robinson, R.L., Stelson, P.H.: Phys. Rev. C10, 1146 (1974)
19. Grodzins, L.: Phys. Lett. 2, 88 (1962)
20. Soloviev, V.G.: Theory of Complex Nuclei. Oxford: Pergamon Press (1976)
21. Paulsen, R.: Ph.D. thesis, University of Bonn (1997)
22. Soloviev, V.G.: Theory of atomic nuclei: Quasiparticles and phonons. Institute of Physics, Bristol and Philadelphia (1992)
23. Soloviev, V.G., Sushkov, A.V., Shirikova, N.Yu.: Phys. Part. Nucl. 25, 157 (1994); 27, 1643 (1996)
24. Soloviev, V.G., Sushkov, A.V., Shirikova, N.Yu.: J. Phys. G 20, 113 (1994)
25. Soloviev, V.G., Sushkov, A.V., Shirikova, N.Yu.: Nucl. Phys. A 568, 244 (1994)
26. Soloviev, V.G., Sushkov, A.V., Shirikova, N.Yu.: Intern. J. Mod. Phys. E 3, 1227 (1994); E 6, 437 (1997)
27. Soloviev, V.G., Sushkov, A.V., Shirikova, N.Yu.: Z. Phys. A 358, 287 (1997)

28. Gallagher, G.J., Moszkowski, S.A.: Phys. Rev. 111, 1282 (1958)
29. Maser, H., Lindenstruth, S., Bauske, I., Beck, O., von Brentano, P., Eckert, T., Friedrichs, H., Heil, R.D., Herzberg, R.-D., Jung, A., Kneissl, U., Margraf, J., Pietralla, N., Pitz, H.H., Wesselborg, C., Zilges, A.: Phys. Rev. C 53, 2749 (1996)
30. Severyukhin, A.B., Sushkov, A.V.: Izv. RAN ser. fiz. 61, 728 (1997)
31. Zilges, A., von Brentano, P., Friedrichs, H., Heil, R.D., Kneissl, U., Lindenstruth, S., Pitz, H.H., Wesselborg, C.: Z. Phys. A 340, 155 (1991)
32. Soloviev, V.G., Sushkov, A.V., Shirikova, N.Yu.: Phys. Rev. C 56, 2528 (1997)
33. Sood, P.C., Gizon, A, Burke, D.G., Singh, B., Liang, C.F., Sheline, R.K., Martin, M.J., Hoff, R.W.: Phys. Rev. C 52, 88 (1995)
34. Sood, P.C., Headly, D.M., Sheline, R.K.: At. Nucl. Data Tables 51, 273 (1992)